# IN VITRO CHARACTERIZATION OF UNMODIFIED AND PYROGLUTAMYLATED ALZHEIMER'S AMYLOID β PEPTIDE

by

JASON MATOS
B.S. University of Puerto Rico at Cayey,
2011

A thesis submitted in partial fulfillment of the requirements
for the degree of Master of Science
in the Burnett School of Biomedical Sciences
in the College of Medicine
at the University of Central Florida
Orlando, Florida

Summer Term
2014

Major Professor: Suren A. Tatulian

# ABSTRACT

Plaques of amyloid β peptide (Aβ) are a hallmark trait of Alzheimer's disease (AD). However, the precise role of Aβ aggregates is not well understood. Recent studies have identified that naturally occurring N-terminal truncation and pyroglutamylation of Aβ significantly increases its neurotoxicity by an unknown mechanism. Content of pyroglutamylated Aβ (pE-Aβ) in AD brains has been shown to reach up to 50% of total Aβ. Modified pE-Aβ co-aggregates with Aβ by a seeding mechanism and forms structurally distinct and highly toxic oligomers. We studied structural transitions of the full-length $Aβ_{1-42}$, its pyroglutamylated form $Aβ_{pE3-42}$, their 9:1 ($Aβ_{1-42}$/$Aβ_{pE3-42}$) and 1:1 molar combinations.

Transmission electron microscopy was used to directly visualize the fibrils of the samples in a buffer mimicking physiological environment. Atomic force microscopy measurements were done to determine rate of second nucleation events in fibrils. Thioflavin-T fluorescence indicated that low ionic strength suppressed the aggregation of $Aβ_{pE3-42}$ but promoted that of $Aβ_{1-42}$, suggesting different paths of fibrillogenesis of unmodified Aβ and pE- Aβ. Interestingly, $Aβ_{pE3-42}$ at only 10% significantly facilitated the fibrillization of $Aβ_{1-42}$ at near-physiological ionic strength but had little effect at low salt.

Circular dichroism and Fourier transform infrared (FTIR) spectroscopy were used to characterize the structural transitions during fibrillogenesis. In aqueous buffer, both unmodified Aβ and pE-Aβ peptides adopted parallel intermolecular β-structure. Interestingly, $Aβ_{pE3-42}$ contained lower β-sheet content than $^{13}C$-$Aβ_{1-42}$, while retaining significantly larger fractions of α-helical and turn structures. Structural details of Aβ and pE-Aβ combinations were unveiled by isotope-edited FTIR spectroscopy, using $^{13}C$-labeled $Aβ_{1-42}$ and unlabeled $Aβ_{pE3-42}$. When exposed to environmental humidity, $Aβ_{pE3-42}$ not only maintained an increased fraction of α-helix but also was able to reverse $^{13}C$-$Aβ_{1-42}$ β-sheet structure. These data provide a novel structural mechanism for pE-Aβ hypertoxicity; pE-Aβ undergoes faster

nucleation due to its increased hydrophobicity, thus promoting formation of smaller, hypertoxic oligomers of partial α-helical structure.

# ACKNOWLEDGMENTS

I want to make special mention of Dr. Suren Tatulian and Dr. Kathleen Nemec. Their unquenchable desire to discover the unknown, and passion to spark this sense in others, made this work possible.

# TABLE OF CONTENTS

# LIST OF FIGURES

# LIST OF ACRONYMS AND ABBREVIATIONS

Adenosine triphosphate (ATP)

Alzheimer's disease (AD)

Amyloid β 1-40 ($A\beta_{1-40}$)

Amyloid β 1-42 ($A\beta_{1-42}$)

Amyloid β peptides (Aβ)

Amyloid precursor protein (APP)

Apolipoprotein E (ApoE)

Atomic force microscopy (AFM)

Cellular prion protein ($PrP^{C}$)

Cerebral amyloid angiopathy (CAA)

Circular dichroism (CD)

Dynamin related protein (Drp1)

Endoplasmic reticulum (ER)

Familial Alzheimer's disease (fAD)

Fission 1 (Fis1)

Fourier transform infrared spectroscopy (FTIR)

Hexafluoroisopropanol (HFIP)

Leukocyte I mmunoglobulin like receptor B (LilrB2)

Neurofibrillar tangles (NFT's)

Phosphatidylinositol (3,4,5)-triphosphate ($PIP_3$)

Pyroglutamylated Amyloid β 3-42 ($A\beta_{pE2-42}$)

Pyroglutamylated Amyloid β peptides (pE-Aβ)

Reactive oxygen species (ROS)

Solid state nuclear magnetic resonance (ssNMR)

Thioflavin T (ThT)

Transmission electron microscopy (TEM)

# CHAPTER ONE: INTRODUCTION

Alzheimer's disease (AD) affects more than 35 million people worldwide, with 5.5 million of those in the United States.[1] Plaques of amyloid β (Aβ) peptide are a hallmark trait of AD. However, the precise role of Aβ aggregates in AD is not well understood. The amyloid cascade hypothesis proposed that extracellular aggregates (plaques) were responsible for the onset of AD.[2, 3] However, recent data identify soluble Aβ oligomers as neurotoxic agents, and show that insoluble, fibrillar aggregates are poorly correlated to brain atrophy.[4-10] Naturally, truncated and pyroglutamylated (pE-Aβ) peptides, such as the pyroglutamylated 40 amino acids long Aβ ($Aβ_{pE3-42}$), have been shown to aggregate at increased rates.[11-13] Recent studies have identified that pyroglutamylation of Aβ significantly increases its neurotoxicity even at low fractions. [14, 15] Interestingly, $Aβ_{pE3-42}$ has been shown to be highly toxic to cultured neurons at the sub-micromolar range and at ≤5% of total Aβ protein.[15] These data suggest that increased toxicity of $Aβ_{pE3-42}$ is through a prion like mechanism. The structural nature of the differences in toxicity remains unknown and was explored in this work. The main objective of this project is to gain insight into the molecular mechanism of altered fibrillogenesis of $Aβ_{1–42}$, by studying the aggregation kinetics and accompanying structural changes in its pyroglutamylated form $Aβ_{pE3-42}$, their 9:1 ($Aβ_{pE3-42}$,$Aβ_{1-42}$), and 1:1 molar combinations. Our data suggest that under certain conditions $Aβ_{pE3-42}$ resists fibrillogenesis and inhibits cross-β structure formation of $Aβ_{1-42}$. This implies that the higher $Aβ_{pE3-42}$ toxicity may be related to its propensity to form low molecular oligomers. We show data collected using a plethora of biophysical techniques, which give new insights into Aβ behavior under physiologically relevant conditions.

## Discovery Of Alzheimer's Disease

The neurological ailment AD is named after German neuropathologist and clinician Aloysius Alzheimer.[16] After receiving his medical degree at the University of Wuzbürg in Lower Fraconia, Germany. He was hired at the Municipal Asylum for the Insane and Epileptic in Frankfurt.[16] This is where he received a patient in which he first identified the disease that bears his name. [16] In 1901 a woman called Auguste Deter was admitted to the hospital and examined by Alzheimer and was found to show a wide array of symptoms such as reduced memory, paranoia and unpredictable behavior.[17] A colleague of Alzheimer, Emil Kraepelin, published in 1910, the 8th edition of his clinical psychiatry textbook in which the term Alzheimer's disease was born.[17]

What Alzheimer first observed in the cerebral cortex of August Deter's brain is probably Aβ peptide aggregates. This peptide is suspected to be a protagonist in the onset and development of AD. The Aβ peptide is found in AD brains and forms large extracellular aggregates called amyloid plaques. The identification of the Aβ led to the study of the disease at a biophysical and biochemical level. Nearly a century after Alzheimer's discovery and initial studies there is no clear established mechanism for the etiology of AD.[18] Nonetheless, there has been some modification of the amyloid cascade hypothesis over the years; current research is shifting towards the toxicity of small soluble oligomers and not insoluble plaques. [5, 6, 19-21]

Identification of The Amyloid β Peptide And Its Pyroglutamated Form

The Aβ peptide has been primarily focused on the study of Alzheimer's disease since it was first identified. This peptide is a cleavage product after β-secretase and γ-secretase act on the Amyloid precursor protein (APP).[22] The most abundant amyloid peptides range from 39 to 42 residues long.[23] The 40 residue amyloid peptide ($A\beta_{1-40}$) and $A\beta_{1-42}$ have been the most extensively studied. However, pE-Aβ such as $A\beta_{pE3-42}$ have received much attention in recent years since its first discovery in 1985.[24] Both $A\beta_{1-42}$ and $A\beta_{pE3-42}$ have been shown to form micron long cross β-sheet fibrils when incubated in aqueous buffer.[25-28] Additionally, there is evidence showing that incubation conditions and presence of seeding species affect final fibril morphology.[28] Previously, fibrillar plaques were thought to have a high correlation with cell toxicity and death.[2, 3] Recent attention is focused on oligomeric species and not fibrils as being the toxic entities.

Determination of the etiology and treatment of AD has increased in complexity since the discovery of post-translationally modified pE-Aβ. Their production occurs when the first two amino acids are truncated by aminopeptidases and glutamate at position three is cyclized by Glutaminyl Cyclase.[14] The loss of two charges increases hydrophobicity and has been shown to cause more rapid aggregation.[29] Even though pE-Aβ have been shown to aggregate at faster rates compared to their unmodified forms, some data shows it to have an inhibitory effect on peptide fibrillization.[30] Indeed, there exists data showing that $A\beta_{1-42}$ aggregates faster than $A\beta_{pE3-42}$.[31] The percentage of $A\beta_{pE3-x}$ has been reported to vary from a few % to more than 50% of total Aβ.[32, 33] It has been suggested that Aβ toxicity depends on peptide ratio and not total Aβ amount.[34]

Evolution Of The Amyloid Cascade Hypothesis

The amyloid cascade hypothesis originally pointed at insoluble extracellular aggregates as the toxic species in AD. Genetic evidence shows a link between a mutation in APP and presenilin and higher risk of developing AD.[35-38] These mutations lead to familial Alzheimer's disease (fAD). Additionally, these mutations are thought to increase the risk of AD by increasing Aβ peptide production. [39] These data suggest a strong link between the onset of AD and higher concentrations of Aβ peptides.

The formation of neurofibrillary tangles made of Tau protein has been shown to be neurotoxic.[40] It has been shown that cultured rat neurons treated with oligomeric Aβ species, displayed translocation from Tau rich axons to dendrites.[41] Alternatively, some studies have identified plaques in brains that do not show pathological Alzheimer's symptoms.[42] In addition, oligomeric species have been found at higher concentration in human brains with cognitive impairment.[43] Finally, it has been suggested that toxicity is detected before plaques are observed in the brain.[5] In fact, there has been data showing that Aβ fibrillar seeds and monomers may be benign or even protective.[44, 45]

These data have led to the modification of the amyloid cascade hypothesis to one in which soluble oligomers like dimers, trimers and dodecamers are the cytotoxic entities.[44, 46-49] Soluble oligomers have been shown to act through several mechanisms such as endoplasmic reticulum (ER) calcium leakage, synaptic loss and have been shown to interact with cell membrane receptors.[50, 51]

Experimental Pitfalls In Previous Aβ Study

Concerns have been raised that non physiological experimental conditions of Aβ studies might have led to incorrect conclusions about its toxic effect.[20] Also, that Aβ peptides have been thought to be associated to other cellular components and hence some studies are too narrow in breadth.[20]Non-physiological conditions such as high ionic strength, acidic and alkaline buffers have been used to determine Aβ behavior. [11, 31] These strategies have given some insight into the fibrillization kinetics of Aβ. Unfortunately, results from a highly varied degree of conditions have also been very diverse. Additionally, increased calcium concentrations have been shown to increase fibrillization rates of Aβ peptides.[52] A group of chaperones identified as "Aβ pathological chaperones" of which Acetylcholinestrase is an example, have been identified.[53] Acetylcholinesterase is thought to aid and increase Aβ fibrillization.[53] Therefore, it is important to provide a more in depth structural and functional description of Aβ peptides.

The aim of this work was to study the effect $A\beta_{pE3-42}$ on $A\beta_{1-42}$ structure and aggregation. By doing this in varying buffer conditions we are able to determine the role of ionic strength on Aβ conformation and fibrillization kinetics. This work also aimed at determining several intermediates during the oligomerization process. Different structural intermediates can help shed light on the structural effects of $A\beta_{pE3-42}$ on $A\beta_{1-42}$ and its role in AD. It is important to emphasize that aggregation and fibrillization kinetics are of high importance in the elucidation of the role of Aβ in AD. Structural characteristics of oligomeric species will probably pave the way to new AD mechanistic understanding. Presently, these "pathological conformations" remain elusive.[54]

# CHAPTER TWO: LITERATURE REVIEW

The interdisciplinary nature of this project required a careful analysis of a large pool of previously published results. AD research is primarily focused on the study of Aβ peptides and the role they play in disease pathology. The molecular aspect of Aβ peptides was researched to gain insight on the current knowledge of their cytotoxic effect on the brain. This information was essential to determine cytotoxicity differences between pyroglutamylated and unmodified Aβ. The ratio of modified to unmodified Aβ peptides was an important piece of data, required for effective design of experimental procedures.

This project employed several techniques which include: i) Fourier transform infrared (FTIR) spectroscopy ii) circular dichroism (CD) iii) aromatic amino acid fluorescence iv) atomic force microscopy (AFM) v) Thioflavin T (ThT) fluorescence assay and vi) transmission electron microscopy (TEM).

Initially our strategy was to determine $A\beta_{pE3-42}$ and $A\beta_{1-42}$ secondary structure in dry, aqueous buffer and organic solvent conditions. Indeed, many structural studies have been done on amyloid peptides such as $A\beta_{1-40.}$[27] Solid-state nuclear magnetic resonance (ssNMR) elucidated the amyloid cross β-sheet structure.[27] These β-sheet rich motifs have been identified in Aβ peptides,[55, 56] and in other proteins related to a variety of diseases[57], such as Huntington's disease,[58] Parkinsons disease,[59] light chain amyloidosis,[60] and Diabetes.[61]

## Alzheimer's Disease Etiology

Aβ peptides are cleavage products from the amyloid precursor protein.[1] Enzymes called β-secretase and γ-secretase cleave Aβ from APP as mentioned above. Mutations in γ-secretase, the active portion of presenilin-1,[62] are associated with fAD, which accounts for <5% of total AD case.[63] It is interesting to note that even though AD was discovered nearly 100 ago there is still no treatments that reverse or stop cognitive decline. There have been many attempts to identify AD causing factors. Apolipoportein E (ApoE), specifically the ε4 allele has been associated with an increased risk of AD when compared to ε2 and ε3 alleles.[64]ApoE has many roles. It has strong binding affinity for Aβ and cholesterol.[65, 66] This can lead to a higher accumulation of Aβ in the intracellular space and also could starve the cell of cholesterol. Certain diet tendencies have also been associated to AD.[67] Some studies have suggested that the intake of omega-3 fatty acids reduces the risk of AD.[68, 69] Moreover, Tau proteins are related to neurofibrillary tangles (NFT's) which are suspected of having a pathological role in AD. Tau proteins are microtubule associated proteins that serve to stabilize microtubules. NFT's form when highly phosphorylated tau aggregates.[70] Other data suggest toxicity of tau oligomers.[71]

AD is associated with advanced age. Specifically, vascular changes and pathologies are associated with aging and AD. Cerebral amyloid angiopathy (CAA), where Aβ peptides are deposited on leptomeningeal and cortical blood vessel walls are associated with aging, AD and other pathological states of vasculature.[72] Calcium homeostasis dysregulation has also been extensively investigated as having a causative role in AD.[73-75] Indeed, data has shown that physiologically relevant calcium concentrations increase $A\beta_{1-42}$ fibrillization

rate.[52] Pore formation capacity on cell plasma membranes of Aβ peptides has also been linked to calcium homeostasis dysregulation [76, 77]

Several mechanisms have been proposed to explain how Aβ peptides elevate calcium levels by pore formation. Neurotoxic species of Aβ have structural and functional homology with pore forming bacterial toxins.[78] The conformation specific antibody A11 binds selectively to $A\beta_{1-42}$ oligomers as well as perforin and α-hemolysin, indicating a similarity in oligomeric structure of pore forming and amyloid peptides.[78] Pores are thought to form on the cell membrane and thus increase influx of calcium into the cytoplasm, thereby rendering the neurons susceptible to excitotoxicity. [73] Other models show pores forming on the ER surface, leading to an increase in calcium concentration in the cytosol. The ER pathway suggest that intracellular Aβ binds to ryanodine receptors, followed by abnormal activation of phospholipase C, which triggers further Phosphatidylinositol (3,4,5)-triphosphate ($PIP_3$)-mediated ER calcium release, leading to apoptotic cell death.[50] In other experiments, $A\beta_{1-42}$ has been shown to promote production of ryanodine receptor mRNA and protein in mice primary cortical neurons.[79] Additionally, Aβ have been shown to cause a calcium dependent cytotoxic effect on rat brain endothelial cells.[80]

Some cell membrane receptors have been shown to bind $A\beta_{1-42}$. Oligomeric $A\beta_{1-42}$ has a high binding affinity for the leukocyte immunoglobulin like receptor B (LilrB2).[51] Mice experiments confirmed that $A\beta_{1-42}$ interacts with PirB, a LilrB2 homolog, and diminishes ocular dominance plasticity.[51] Aβ soluble oligomers have also been shown to bind with high affinity to lipid anchored cellular prion protein ($PrP^c$) on the postsynaptic density. [81]The mGluR5 transmembrane receptor links $PrP^c$ to an intracellular kinase called Fyn; downstream effects promote dendritic loss.[81]

Phosphatidylserine exposure increases Aβ ability to associate to the cell membrane. [82] It is possible that age related mitochondrial defects increase phosphatidylserine content on the outer cell membrane. Decreased cytosolic adenosine triphosphate (ATP) and the presence of cells in G1 stage had positive correlation with Aβ binding and an increased cytosolic calcium concentration. [82] Moreover, data has shown that $A\beta_{1-42}$ cytotoxicity is affected by membrane cholesterol concentration.[83-85] Some experiments show that cholesterol deficient plasma membranes are more susceptible to toxic effect of Aβ.[83] While others state that increased cholesterol content facilitates Aβ toxicity.[86]

Mitochondria impairments have been linked to AD.[87, 88] With increased age there is an increase in mitochondria oxidative stress.[89] Reactive oxygen species (ROS) generated from mitochondria increase Aβ formation. [89] Interestingly, Aβ has been found in mitochondria of AD in both monomeric and oligomeric forms.[89] This suggests a role of Aβ in mitochondrial related defects in AD . The electron transport chain is involved in producing the cell's energy in form of ATP. Oxygen is the final electron acceptor and is subsequently reduced to water. In this process ROS can oxidize lipids, mitochondrial DNA, and proteins which in turn increase mitochondrial degeneration.[90] Excessive mitochondrial fission has been observed in AD, this may lead to dysfunction in mitochondria and thus impaired neurons. Intraneuronal Aβ has been show to bind to fission related dynamin related protein (Drp1).[91] Mitochondrial fission genes expressing Drp1 and fission 1 (Fis1) have been shown to be upregulatd in AD brains.[91] This probably leads to an imbalance in mitochondrial dynamics which can lead to cell death.

## Aβ And pEAβ Comparison

With the discovery of pyroglutamylated amyloid peptides arose a need to determine its cytotoxic effect and shed light on its role in AD. After cleavage from APP, the N-terminal aspartate and alanine are nonspecifically truncated by intracellular aminopeptidases, followed by cyclization of glutamates at position 3. Loss of two charges (the N-terminal primary amine and the Glu3 side chain carboxyl) increases hydrophobicity; faster aggregation kinetics have been observed for $A\beta_{pE3-42}$. Concentrations of pyroglutamylated Aβ in the AD brain have been shown to reach 50% of total Aβ.

Data suggest that the ratio of Aβ and pEAβ has a significant effect on cytotoxicity and aggregation kinetics.[25, 30] A literature search of fibrillization studies resulted in conflicting data. Some reports showed pEAβ to aggregate faster than $A\beta_{1-42}$,[11, 30, 92] while others showed the opposite [31] Importantly, one group has reported that $A\beta_{pE3-42}$ inhibits $A\beta_{1-42}$ fibrillization and cross β-sheet formation by TEM studies.[30] Pyroglutamylation of Aβ increases resistance to aminopeptidases and astrocyte induced degradation.[25] Even though there has been extensive studies comparing $A\beta_{1-42}$ and $A\beta_{pE3-42}$, an understanding in unique features in the structural effect of $A\beta_{pE3-42}$ on $A\beta_{1-42}$ has not been reached. Our work aims to elucidate these features under physiologically relevant conditions.

Methodology literature review

This project applied a wide array of biophysical techniques. Protocols will be discussed in the methods chapter and only a brief overview of searched literature is provided below. We followed a careful series of steps to elucidate the fibrillization kinetics, peptide secondary structure and fibril morphology. The effect of ionic strength on structure and fibrillization was also studied. ThT binding assays probed fibril formation in solution. ThT has been shown to fluoresce in the visible range when bound to cross β-sheet structure formed by fibrils.[93-95]

Previously published data helped us develop optimal ThT concentrations. We employed CD, FTIR, and isotope edited FTIR to investigate secondary structure and interactions between $A\beta_{1-42}$ and $A\beta_{pE3-42}$. Interpretation of CD spectra was aided by searching previous published protocols.[96] Positions of secondary structure components in the infrared Amide I region were researched.[97] Importantly, the effect of $^{13}C$ isotope presence in peptide was reviewed to help determine shift in Amide I.[98, 99]

Fibril morphology was probed by TEM and AFM. Preparation of fibrils and amyloid aggregates was researched.[28, 100-103] Optimal buffer conditions were also determined. TEM and AFM substrates were carefully selected for sample preparation. We used graphene coated grids for TEM which provide superior resolution of amyloid peptides.[104] Mica was the substrate used for AFM.

# CHAPTER THREE: RESEARCH METHODS

This work aims to determine the secondary structure and the strength of association between $A\beta_{pE3-42}$ and $A\beta_{1-42}$ in dry, aqueous buffer and intermediate conformations. Isotope edited FTIR is an ideal approach for this purpose. Subsequently, the effect of $A\beta_{pE3-42}$ on $A\beta_{1-42}$ fibril formation determined by ThT will be investigated. Finally, fibril morphology will be probed by TEM and AFM measurements. Our experimental samples consisted of $A\beta_{1-42}$, $A\beta_{pE3-42}$, their 9:1 ($A\beta_{1-42}/A\beta_{pE3-42}$) and their 1:1 molar combinations. Aβ peptides adopt a α-helical conformation in HFIP. [105, 106] Moreover, fluorinated alcohols have been shown to break up aggregates and promote monomeric state of Aβ peptides.[105, 106] CD proved to be optimal when estimating peptide secondary structure in HFIP. FTIR showed secondary structure of desiccated peptides and in bulk aqueous buffer. By $^{13}C$ uniform labeling of $A\beta_{1-42}$ we are able to dissect peptide mixtures when this peptides is combined with unlabeled $A\beta_{pE3-42}$. This is achieved since $^{13}C$ labeled peptides show a downshift of the Amide I band of ~45 $cm^{-1}$.

By following ThT fluorescence we were able to study fibril formation from a monomeric state. Our experiments were done under two buffer conditions i) 50 mM phosphate and 50 mM sodium chloride, at pH 7.2 and ii) 10 mM phosphate at pH 7.2. These buffer conditions were selected to determine the effect of ionic strength on peptide structure and fibrillization kinetics. TEM and AFM were performed to determine characteristic differences between fibrils and to identify second nucleation sites. Combining data from these techniques permitted the careful study of $A\beta_{1-42}$ and $A\beta_{pE3-42}$ behavior under varying conditions. Below there is a detailed description of the conditions and procedures used to collect and analyze the data presented in this project.

## Secondary Structure And Fibrillization Kinetics Studies

Secondary structure of peptides was determined using CD and FTIR. Peptides secondary structure is of upmost importance in determining protein behavior, interaction with their surroundings, and function. Initially, peptides were dissolved in HFIP to disperse previously formed aggregates. To remove HFIP, samples were gently dried with a stream of nitrogen and vacuum desiccated for 15 minutes. The CD measurements were performed on Aβ peptides using 4mm quartz cuvettes and measured using a Jasco J-810 spectropolarimeter with a fluorescence attachment (Tokyo, Japan). ThT binding assay was taken simultaneously with CD. Both buffer conditions mentioned above were used for comparing the effect of salt on Aβ behavior.

CD was measured in HFIP dissolved peptides using a 0.5 mm cylindrical cuvette. Measurements in buffers were performed on 50 μM solutions over a time span of 24 hours, while gently stirring. CD spectra were measured ranging from 180 nm to 330 nm. ThT was excited at 440 nm and emission was recorded from 430 nm to 540 nm. Maximum intensity vs. time graphs were plotted. In the case for ThT the emission maximum was determined to be 483 nm and was baseline corrected by subtraction of the signal at 540 nm.

Further structural assessment was achieved by isotope edited FTIR. The spectra were measured on a Vector-22 FTIR spectrometer (Bruker Optics, Billerica, MA, USA) equipped with a liquid nitrogen-cooled Hg-Cd-Te detector, at 2 $cm^{-1}$ nominal resolution. Measurements were taken using two peptide stock concentrations in HFIP. First, $^{13}C$ labeled $A\beta_{1\text{-}42}$ and $A\beta_{pE3\text{-}42}$ were dissolved at 200 μM in HFIP. Forty μL of each peptide and their 9:1 and 1:1 mixtures were placed on a $CaF_2$ FTIR window and then desiccated for 15 minutes to remove

residual HFIP. Transmission spectra in buffer were taken using 1000 consecutive scans while dry samples were taken using 500 scans and absorption was calculated using appropriate reference transmission spectra.

Samples containing peptides by themselves and in mixture were exposed to air to determine the effect of moisture on the secondary structure. Presence of increased moisture was confirmed by the increase in the $H_2O$ stretching bands near 3,200 $cm^{-1}$.[97]

Subsequently peptide stocks were made at 50 μM in HFIP. Secondary structure for these samples was probed under two different bulk buffer conditions mentioned above. Eighty μL of peptide solution were dried and desiccated as mentioned above. After measuring dry spectra 80 μL of bulk $D_2O$ buffers were added and samples were sandwiched between 2 $CaF_2$ windows using a 50 μm Teflon spacer, and measured using 1000 scans for several hours to observe changes in secondary structure. The pD of $D_2O$ buffers was 6.8 corresponding to pH 7.2. $D_2O$ is used instead of $H_2O$ because $H_2O$ absorbs in the amide I region and obscures the protein signal.[107] Reference spectra for both buffers were taken in a similar fashion without the presence of peptide for calculation of absorption spectra.

## Fibril Morphology by TEM and AFM

TEM and AFM measurements were performed to probe Aβ fibril and aggregate morphology. For TEM, peptides were dissolved in HFIP and dried as described above. Dried peptide film was resuspended to 50 μM using 50 mM phosphate with 50 mM NaCl buffer at pH 7.2. Samples were stirred at 37$^{o}$C for 24 hours. Five μL of peptide preparations were placed on graphene coated grids. After 5 minutes excess water was wicked off. Samples were washed twice with di$H_2O$, and were negatively stained with 3% uranyl acetate. After washing, samples were measured using a JEOL TEM-1011 (Tokyo, Japan) operated at 80kV. Data was collected at several time points 2,4,12 and 24 hours to determine aggregation and fibrillization states of peptides.

AFM sample preparation was similar to TEM. After 24-hour incubation, 25 μL of fibril preparation was placed on freshly cleaved mica. Mica was incubated for 24 hours to let fibrils adsorb to the substrate. Then mica was washed with ultra-pure water and vacuum desiccated for 15 minutes. Measurements were taken using a Dimension 5000 Atomic Force Microscope system (Digital instruments, Santa Barbara, Ca, USA) equipped with a silicon tip with a length of 160 mm, thickness of 4.6 mm, and width 45mm. Amplitude and height profiles helped elucidate fibril morphological characteristics.

# CHAPTER FOUR: RESULTS

In this work we examined $A\beta_{1-42}$, $A\beta_{pE3-42}$, their 9:1 ($A\beta_{1-42}/A\beta_{pE3-42}$) and 1:1 molar combinations. Previous data have shown that Aβ oligomeric mixtures containing low % of $A\beta_{pE3-42}$, have increased neurotoxicity when compared to $A\beta_{1-42}$ alone, and are structurally distinct.[15] This suggests that differences in toxicity levels are related to Aβ oligomer secondary structure. We hypothesized that $A\beta_{pE3-42}$ and $A\beta_{1-42}$ have strong intermolecular interactions in buffer.

Both $A\beta_{1-42}$ and $A\beta_{pE3-42}$ aggregate into amyloid fibrils. Some disagreements have arisen concerning which has increased fibrillization rate. Some data show that $A\beta_{1-42}$ fibrillizes faster than $A\beta_{pE3-42}$,[31] while others point to the opposite.[11] Aggregation pathways are of significance, since intermediate oligomeric species and not mature amyloid fibrils are thought to be the neurotoxic entities in AD.[108] Some data suggest that mature fibrils might be neuroprotective, by sequestration of monomers, and thus inhibition of oligomer formation.[109] In our studies we focused on the effect of salt concentrations on Aβ structure and fibrillization. Based on these data we hypothesized that varying buffer conditions promote diverse trends in aggregation.

Data from this project resulted in significant advancements in the understanding of Aβ peptides, which can be divided into two main ideas. $A\beta_{pE3-42}$ affects $A\beta_{1-42}$ structure and fibrillization kinetics when combined at disease relevant ratios. Secondly, ionic strength plays a determining role in Aβ structure and aggregation.

Strong solvents such as HFIP have been reported to promote monomeric state of Aβ peptides.[110] In HFIP $A\beta_{1-42}$ has been shown to be in α-helical and unordered conformations.[111] Peptide samples in α-helical conformation show negative minima around 222 nm and 208 nm.[112] Unordered structures are characterized by a strong negative band near 200 nm.[112] CD spectra confirmed α-helical and unordered secondary structures for all samples in HFIP (**fig. 1 a**). Additionally, $A\beta_{pE3-42}$ shows a reduced ratio of ellipticities, $\theta_{208}/\theta_{222,}$ this indicates a more flexible, unordered α-helix.[113] The α-helical conformation is present after desiccation as seen in (**fig. 1 b**). This permits us to follow fibrillization from initial non-aggregated states.

Presence of bulk aqueous buffer promotes structural changes on Aβ samples and their combinations (**fig. 1 c**).Both $A\beta_{1-42}$ and the 9:1 combination show a negative band around 218, corresponding to β-sheet structure.[96] Wider and broader negative bands for $A\beta_{pE3-42}$ and the 1:1 combination suggest a combination of α-helix with β-sheet.[114] Interestingly, a higher molar concentration of $A\beta_{pE3-42}$ reduces β-sheet propensity and is similar to $A\beta_{pE3-42}$ by itself, as shown by the 1:1 combination spectrum. Our data show that $A\beta_{1-42}$ and $A\beta_{pE3-42}$ contain distinct structural features in buffer. Additionally, at equimolar concentrations $A\beta_{pE3-42}$ is able to transmit structural features to $A\beta_{1-42,}$ and promote a more helical conformation, by decreasing β-sheet content.

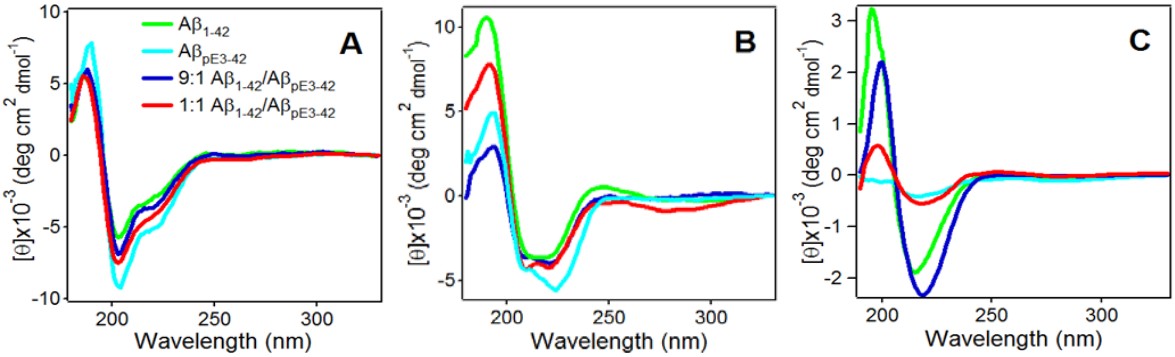


Figure 1. CD spectra of $A\beta_{1\text{-}42}$ (green), $A\beta_{pE3\text{-}42}$ ( light blue), 9:1 $A\beta_{1\text{-}42}/A\beta_{pE3\text{-}42}$ (blue) and 1:1 (red) peptide combinations in HFIP (A), desiccated (B), and bulk buffer (C) conditions. Buffer composition is 10 mM Na,K-phosphate at pH 7.2.

For further elucidation of unique structural features of individual and mixed Aβ peptides, isotope edited FTIR was employed. Uniform isotope enrichment of the backbone carbons of $A\beta_{1\text{-}42}$ produces a spectral downshift of ~45 $cm^{-1}$. In buffer conditions $^{13}C\text{-}A\beta_{1\text{-}42}$ shows prominent intermolecular β-sheet structure as evidenced by a peak around 1585 $cm^{-1}$ (**fig. 2 blue line**). In bulk buffer conditions $A\beta_{pE3\text{-}42}$ shows absorbance around 1628 $cm^{-1}$ corresponding to β-sheet (**fig. 2 red line**). Interestingly, the pyroglutamylated peptide also shows significant absorbance ranging from 1650 to 1680 $cm^{-1}$. This indicates that $A\beta_{pE3\text{-}42}$ is in partial α-helical conformation, while $A\beta_{1\text{-}42}$ is mostly β-sheet. The amide II provides additional structural information. Open, or solvent accessible tertiary structures undergo rapid hydrogen/deuterium exchange. This results in reduction of the amide II band at ~1540 $cm^{-1}$.[115] Data from figure 2 shows that $^{13}C\text{-}A\beta_{1\text{-}42}$ retains significant absorption at the amide II band. This suggests that $^{13}C\text{-}A\beta_{1\text{-}42}$ forms tight tertiary structure. Tight intermolecular β-sheets are indicative of fibril cross β-sheet structure.[116, 117] Conversely, $A\beta_{pE3\text{-}42}$ forms an open solvent accessible structure, shown by a loss of amide II absorption. These data agree with the CD data in figure 1. Unmodified $A\beta_{1\text{-}42}$ forms tight intermolecular β-sheet, while

$A\beta_{pE3\text{-}42}$ forms an open solvent accessible partially α-helical structure. These data suggest that partial α-helical structures and not fibril cross β-sheet are the hypertoxic species in AD.

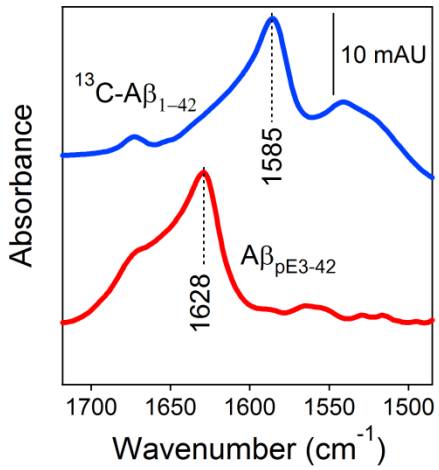


Figure 2. FTIR spectra $A\beta_{pE3\text{-}42}$ (red line) and $^{13}$C-$A\beta_{1\text{-}42}$ (blue line) in 10 mM Na,K Phosphate buffer (pD 7.2). Peptide concentration is 100 μM.

Further FTIR measurements were performed at 50 μM, on desiccated peptide samples. Presence of α-helical conformation after HFIP desiccation was probed. Spectra for $A\beta_{1\text{-}42}$ and $A\beta_{pE3\text{-}42}$ show predominant α-helical peak around 1658 cm$^{-1}$ as shown in (**fig. 3 a,b**). Spectra of both 9:1 ($^{13}$C-$A\beta_{1\text{-}42}$/$A\beta_{pE3\text{-}42}$) (**fig. 3 c**) and 1:1 ($^{13}$C-$A\beta_{1\text{-}42}$/$A\beta_{pE3\text{-}42}$) (**fig. 3 d**) show prominent α-helical component belonging to $A\beta_{pE3\text{-}42}$ near 1660 cm$^{-1}$. In the 9:1 combination the peak at 1618 cm$^{-1}$ shows the α-helical structure of isotope enriched $^{13}$C-$A\beta_{1\text{-}42}$. Conversely, the absorption profile of the sample with equimolar peptide concentrations shows a peak at around 1604 cm$^{-1}$. This peak is probably irregular secondary structure of $^{13}$C-$A\beta_{1\text{-}42}$. This low frequency component difference in the combination measurements led us to explore the possibility that hydration levels or varying peptide ratios exerted an effect on amyloid secondary structure. Aβ peptides absorb atmospheric humidity, which results in $H_2O$ stretching and increase in intensity at ~3270 cm$^{-1}$.[97] Humidity exposure of combinations

helped determine if conformational changes were caused by peptide interactions and/or exposure to moisture. As shown in (**fig. 4**) $A\beta_{1\text{-}42}$ contains the highest amount of humidity followed by the 1:1 combination; $A\beta_{pE3\text{-}42}$ and the 9:1 contain the lowest and a very similar amount of humidity. The 1:1 combination and $A\beta_{1\text{-}42}$ show different secondary structure components while having similar amounts of humidity. These data motivated experiments where the effect of $A\beta_{pE3\text{-}42}$ on $A\beta_{1\text{-}42}$ structure was investigated in bulk buffer conditions at 10% and 50% $A\beta_{pE3\text{-}42}$.

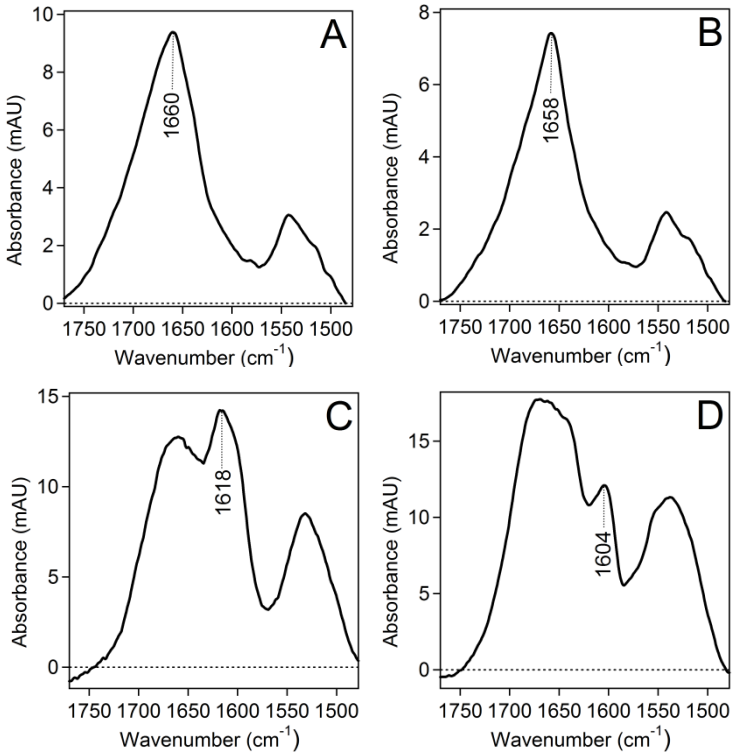


Figure 3. FTIR of desiccated $A\beta_{1\text{-}42}$ (A), $A\beta_{pE3\text{-}42}$ (B), 9:1 ($^{13}C\text{-}A\beta_{1\text{-}42}/A\beta_{pE3\text{-}42}$) (C), and 1:1 ($^{13}C\text{-}A\beta_{1\text{-}42}/A\beta_{pE3\text{-}42}$) (D) molar combinations. Peptide dried from a 50 μM stock.

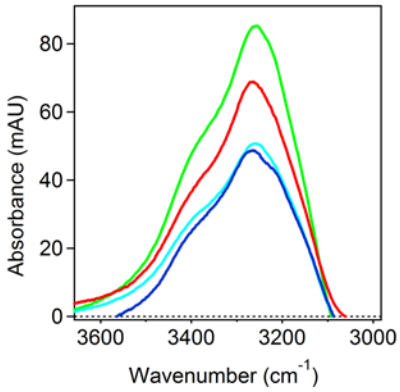


Figure 4. $H_2O$ stretching mode of $A\beta_{1\text{-}42}$ (green), $A\beta_{pE3\text{-}42}$ (light blue), their 9:1 (blue) and 1:1 (red) molar combinations under desiccated conditions.

Interpretation of previously published toxicity data led us to hypothesize that $A\beta_{pE3\text{-}42}$ interacts strongly with $A\beta_{1\text{-}42}$. Dot blot experiments showed that oligomers of $A\beta_{1\text{-}42}$ and $A\beta_{pE3\text{-}42}$ combinations are in distinct structural conformations, when compared to single peptide oligomers.[15] We hypothesized that combining $A\beta_{1\text{-}42}$ and $A\beta_{pE3\text{-}42}$ affects their secondary structure. FTIR was employed pursuing two specific goals. First, determine that $A\beta_{pE3\text{-}42}$ and $^{13}C\text{-}A\beta_{1\text{-}42}$ have close intermolecular interactions. Secondly, probe the structural effects of the pyroglutamylated peptide on the unmodified Aβ.

We studied the effect of $A\beta_{pE3\text{-}42}$ at 10% and 50% total peptide content. To determine the presence of intermolecular interactions we compared the mixture spectra to the weighted average sum spectra of the peptides by themselves. At 10% $A\beta_{pE3\text{-}42}$ the β-sheet peak at 1585 for $^{13}C\text{-}A\beta_{1\text{-}42}$ is upshifted by 3 $cm^{-1}$, and by 10 $cm^{-1}$ at equimolar concentrations (**fig. 5 a**). The β-sheet component around 1626 $cm^{-1}$ for $A\beta_{pE3\text{-}42}$ upshifts by 10 and by 4 $cm^{-1}$ when at 10% and 50% total peptide, respectively. This shows strong vibrational coupling between both species, implying that $A\beta_{pE3\text{-}42}$ and $A\beta_{1\text{-}42}$ form mixed β-sheet structures with strong

intermolecular interactions. Additionally, at equimolar concentrations the averaged sum shows significantly larger turn component (**fig. 5 b**), evidenced by increase absorption near 1671 $cm^{-1}$, when compared to the mixture spectra.

Transition of Aβ peptides from α-helical when dry to β-sheet when exposed to buffer led us to hypothesize that exposure to environmental humidity would have an effect of peptide secondary structure. These data could shed light on intermediate conformations preceding fibrillar cross β-sheet structure. Structural effects were probed by exposing 9:1 ($^{13}$C-A$\beta_{1-42}$/A$\beta_{pE3-42}$) and 1:1 molar combinations to environmental humidity for established periods of time. And infrared measurements were collected.

The initial 9:1 combination spectra taken after 10 minutes of incubation is dominated by the spectral features of the $^{13}$C-A$\beta_{1-42}$ i.e. α-helical at 1617 cm-$^{1}$ and β-sheet component at 1592 $cm^{-1}$ (**fig. 6 a**). The peak at 1655 $cm^{-1}$ represents the α-helical component of the A$\beta_{pE3-42}$. The 20 minute spectrum shows a α-to-β transition of the $^{13}$CA$\beta_{1-42}$ as shown by blue line. Strikingly, the β-sheet content in the 20 minutes incubated sample is lower than expected without the interaction of the peptides ( the weighted sum of the individual spectra incubated for 15 minutes represented by the green line). This data suggest that A$\beta_{pE3-42}$ slows down fibrillization at 10% total Aβ.

.

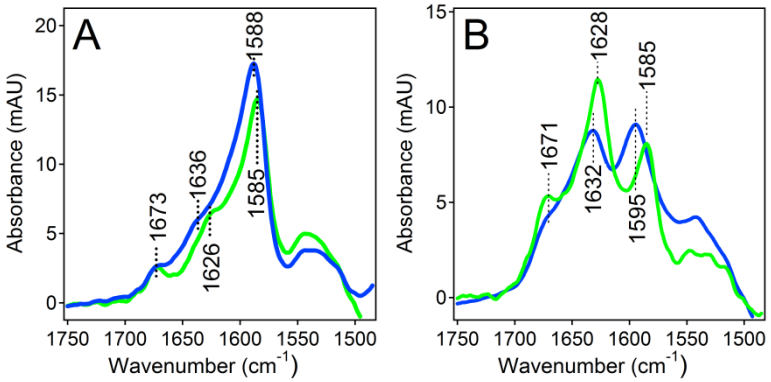


Figure 5. FTIR spectra of $^{13}CA\beta_{1-42}$ and $A\beta_{pE3-42}$ combined at 9:1 (A) and 1:1 (B) molar ratios, incubated in a $D_2O$-based 10 mM Na,K phosphate buffer (pD 7.2) for 2 h, at a total peptide concentration of 100 μM. Blue and green lines are the experimental spectra obtained on the two peptides combined in one sample and the weighted sums of individual spectra, respectively. The weighted sums were obtained as $A = \Sigma fiAi$, where *fi* is the molar fraction and *Ai* is the absorbance spectrum of each individual peptide measured separately.

Moreover, at a 1:1 combination, $A\beta_{pE3-42}$ reverses fibrillization evidenced by the reduction of the $^{13}CA\beta_{1-42}$ β-sheet signal at 1595 $cm^{-1}$ (**fig. 6 b green line**). The sample exposed to environmental humidity for twenty minutes (**fig. 6 b blue line**) shows strong absorption near 1658 $cm^{-1}$, corresponding to the α-helical component of $A\beta_{pE3-42}$ with some contribution from the turn components of the unmodified peptide. Most importantly, there is no α-helix to β-sheet conversion of the $A\beta_{1-42}$ when combined with $A\beta_{pE3-42}$ at equimolar concentrations, as shown by similar signal intensity at 1617 $cm^{-1}$ after 10 and 20 minutes of incubation.

In fact, β-sheet present at 10 minutes is reversed. Our data imply that at 10% $A\beta_{pE3-42}$ the fibrillization process is slowed down. When $A\beta_{pE3-42}$ and $^{13}CA\beta_{1-42}$ are incubated at equal ratios the fibrillization process is completely inhibited, and reversible, while α-helical structure is promoted.

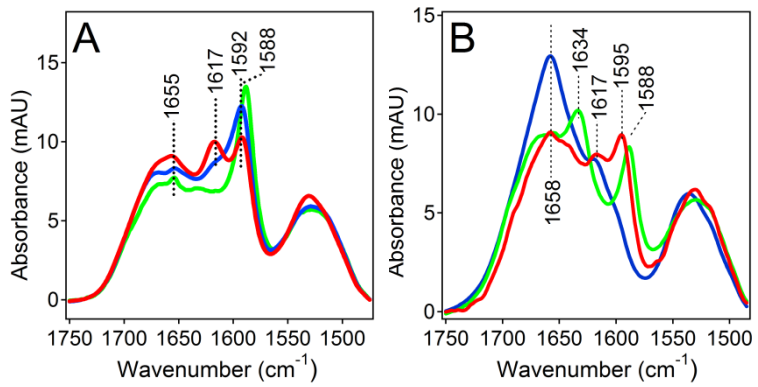


Figure 6. FTIR spectra of humidified Aβ at a 9:1 ($^{13}$C-Aβ$_{1-42}$/Aβ$_{pE3-42}$) (A) and 1:1 ($^{13}$C-Aβ$_{1-42}$/Aβ$_{pE3-42}$) (B) combinations. Red and blue lines are experimental spectra of desiccated HFIP samples followed by exposure to atmosphere for 10 and 20 minutes, respectively. The green spectrum is the weighted sum of the spectra of each combination measured individually, exposed to the atmosphere for 15 minutes.

Additionally, strong intermolecular interaction between the peptides is shown by a frequency shift of the β-sheet component of $^{13}$C-Aβ$_{1-42}$ from 1588 to 1592 cm$^{-1}$ for the 9:1 combination and to 1595 cm$^{-1}$ for the 1:1 combination. These data suggest that Aβ$_{pE3-42}$ might shift aggregation pathway to the formation of partial α-helical intermediates by direct intermolecular interactions with the unmodified peptide. Continuing from this interesting finding, we attempted to determine the structural effect of humidification of the Aβ$_{pE3-42}$/$^{13}$C-Aβ$_{1-42}$ combination with $D_2O$ vapor. By exposing a 1:1 Aβ combination we are able to probe gradual structural changes that happen in an undetectable time frame when bulk buffer is added to dried samples. To achieve this we used a nitrogen tank that blew nitrogen gas through four Erlenmeyer flasks that contained $D_2O$ heated to a moderately simmering temperature followed by delivery of the $D_2O$-saturated gas to the infrared spectrometer containing the peptide samples.

While $D_2O$ traveled through the instrument chamber FTIR spectra were taken every 10 minutes. Thereafter, the sample was left in the instrument chamber without humidification for 24 hours. Finally, the $CaF_2$ window containing the sample was left exposed to environmental humidity for 3 days. The initial absorption spectra corresponding to the desiccated sample with no humidity exposure shows prominent α-helical structure of both $^{13}C$-$A\beta_{1-42}$ and $A\beta_{pE3-42}$ (**fig. 7 black line**). This is evidenced by the prominent peak near 1657 $cm^{-1}$ for $A\beta_{pE3-42}$ and at 1617 for $^{13}C$-$A\beta_{1-42}$. Even under desiccated conditions there is some β-sheet component, showed by a small shoulder at 1598 $cm^{-1}$.Exposure to humidification by $D_2O$ initiates β-sheet formation of the $^{13}C$-$A\beta_{1-42}$ as evidenced by an increase in the 1598 $cm^{-1}$ peak with a decrease in the 1617 $cm^{-1}$. The $A\beta_{pE3-42}$ α-helical component decreases while absorbance increases near 1628 $cm^{-1}$, corresponding to β-sheet formation. Strikingly, after humidity was removed from instrument sample chamber and purged dry air for 24 hours there was an increase in native β-sheet secondary structure of $A\beta_{pE3-42}$. This is evidenced by an increase in intensity of the component at 1639 $cm^{-1}$ (**fig. 7 blue line**). After 3 days of environmental exposure this component approaches a more unordered structure by increasing to 1646 $cm^{-1}$. This data show that the $A\beta_{pE3-42}$ has very dynamic structural transitions when exposed to varying amounts of humidity.

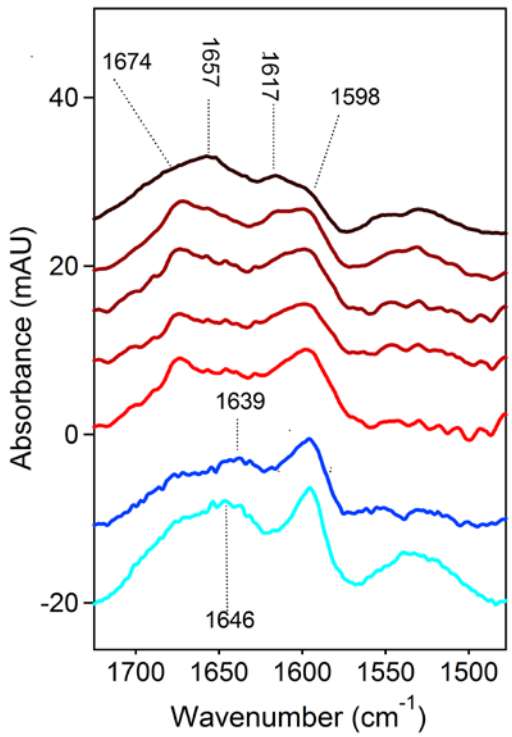


Figure 7. $^{13}$C-A$\beta_{1\text{-}42}$ and A$\beta_{pE3\text{-}42}$ combined at a 1:1 molar ratio desiccated from HFIP (black line) and exposed to $D_2O$-saturated nitrogen gas while spectra were taken every 10 minutes (decreasing red line darkness). Sample was left in the instrument chamber while purging with dry air for 1 day (blue line). Subsequently, sample was exposed to environmental humidity for 3 days (light blue line). Total peptide concentration was 50 μM.

These experiments were conducted with peptides from 50 μM stocks, while samples from figure 6 were from 200 μM stocks. Our data show that humidity, Aβ mixture ratio and initial stock concentrations could affect peptide behavior and oligomerization pathways, by modifying secondary structure.

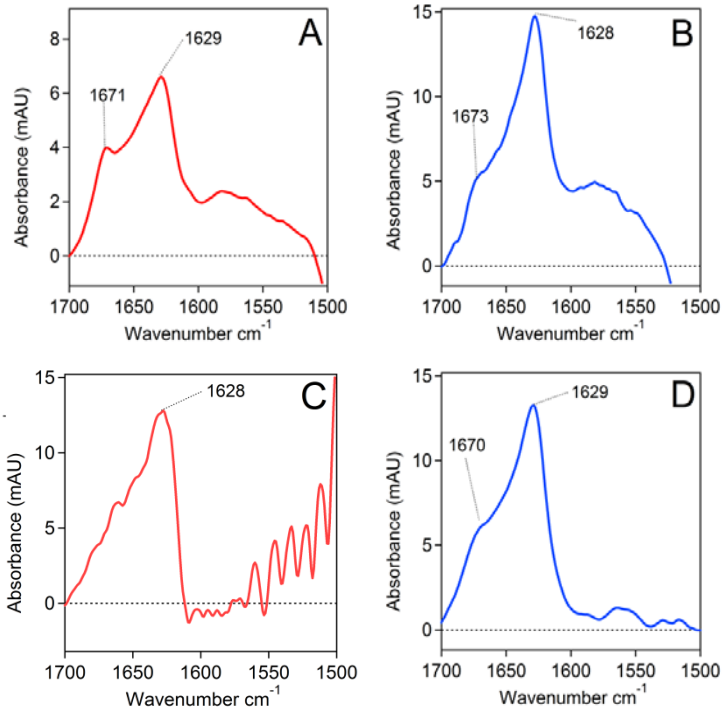


Figure 8. FTIR spectra of 50 μM $A\beta_{1\text{-}42}$ in 50 mM NaCl + 50 mM Na,K-phosphate (pD 7.2) (A) and at 10 mM Na,K phosphate (pD 7.2) (B), and $A\beta_{pE3\text{-}42}$ in 50 mM NaCl + 50 mM Na,K-phosphate (pD 7.2) (C) and 10 mM Na,K-phosphate (pD 7.2) (D).

Previous experiments report that $A\beta_{1\text{-}42}$ aggregates more readily than $A\beta_{pE3\text{-}42}$.[31] Others report that $A\beta_{pE3\text{-}42}$ fibrillizes faster.[11] This led us to investigate the secondary structure of different Aβ peptides and their combinations under both high and low ionic strengths, to determine if variations in fibrillization pathways were caused by initial secondary structure differences. Additionally, oligomeric structure of Aβ peptide mixtures could lead to advancements in rational drug design, aiming at prevention and treatment of AD.

To determine if the initial secondary structure have unique characteristics we have employed FTIR on both $A\beta_{1-42}$ and $A\beta_{pE3-42}$ as shown in figure 8. Ionic strength plays an important role on fibrillization kinetics and both low and high salt conditions were probed in these studies. At both salt concentrations $A\beta_{1-42}$ displays a prominent β-sheet component, evidenced by a strong absorption band at ~ 1628 $cm^{-1}$ **(fig. 8 a,b)**. Interestingly, close to physiological salt concentrations **(fig. 8 a)** $A\beta_{1-42}$ shows a higher turn to sheet ratio when compared to low ionic strength **(fig. 8 b)**, evidenced by a more intense turn component at ~1671 $cm^{-1}$.

In Both high and low salt concentrations, $A\beta_{pE3-42}$ shows prominent β-sheet signature and a turn component, shown by a strong absorption peak at ~1628 $cm^{-1}$, and a weaker component at 1671$cm^{-1}$ (**fig. 8 c,d**), respectively. Salt concentrations have no effect on tertiary structure and compactness of either peptide in aqueous environments as shown by constant amide II intensities at ~1540 $cm^{-1}$. In both cases $A\beta_{1-42}$ shows a strong Amide II band, pointing at a compact tertiary structure. Conversely, $A\beta_{pE3-42}$ shows a more solvent accessible tertiary structure shown by a lack of absorption in the Amide II region. Interestingly, ionic strength has a significant effect on $A\beta_{1-42}$ secondary structure which helps give molecular insight into differences seen in fibrillization rate and final aggregate/fibril morphology. Differences in secondary and tertiary structure help explain varying rates of fibrillization and varied fibril morphology observed by TEM and AFM (see below).

Similar experiments were conducted on the 9:1 $A\beta_{1-42}/A\beta_{pE3-42}$ ($^{13}C$-$A\beta_{1-42}/A\beta_{pE3-42}$) and 1:1 combinations. By employing Isotope labeled FTIR distinct structural features of each peptide were obtained. At a 9:1 at both low and high salt concentrations the peptide mixture shows strong intermolecular β-sheet evidenced by absorbance at 1590 $cm^{-1}$ (**fig. 9 a,b)**. This peak corresponds to vibrational modes between $^{13}C$-$A\beta_{1-42}$ and $A\beta_{pE3-42}$. The component at ~ 1638 $cm^{-1}$ is more prominent under high ionic strength conditions and probably belongs to the β-sheet component of $A\beta_{pE3-42.}$ This component represents ~44% of the height of the component at ~1590 $cm^{-1}$ for high salt concentrations and ~32% for low ionic strength conditions. These data suggest that higher ionic strength better promotes β-sheet of the pyroglutamated form.

At equimolar peptide concentrations there are prominent β-sheets peaks at ~1633 $cm^{-1}$ for the pyroglutamylated peptide and at ~1596 $cm^{-1}$ for the hybrid β-sheets. The higher frequency for the component under 1600 $cm^{-1}$ indicates strong $^{12}C$-$^{13}C$ vibrational coupling. This indicates a larger interaction and hybridization between both labeled and unlabeled peptides.

Interestingly, variations in salt concentrations affected the tertiary structure of both samples. At a 9:1 ratio there is a less compact tertiary structure under low ionic strength as shown by the amide II band at ~1540 $cm^{-1}$ **(fig. 9 b)**. While at a 1:1 ratio lower salt retains higher amide II signal and thus shows a more compact and less solvent accessible structure.

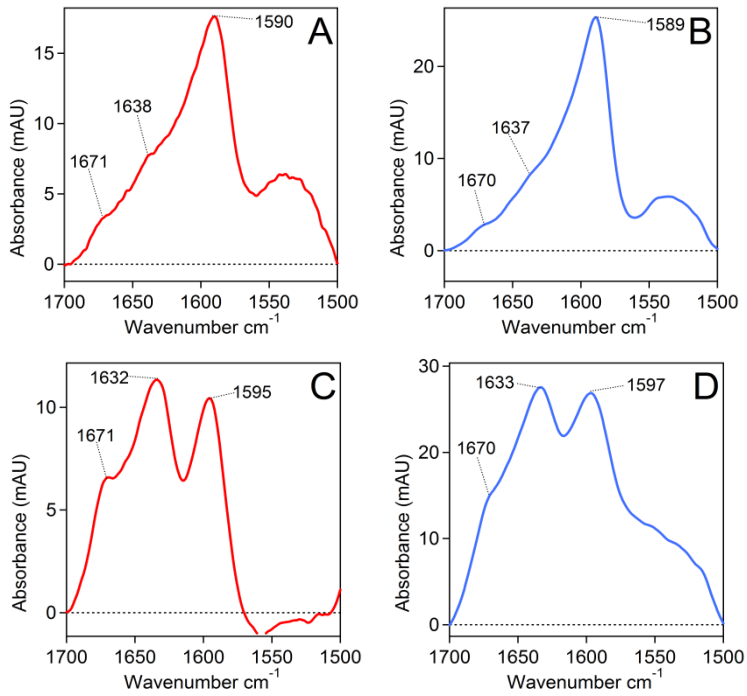


Figure 9. FTIR spectra of 9:1 50 μM ($^{13}$C-Aβ$_{1-42}$/Aβ$_{pE3-42}$) in 50 mM NaCl + 50 mM Na,K phosphate (pD 7.2) (A) and at 10 mM Na,K phosphate buffers (pD 7.2) (B), and 1:1 ($^{13}$C-Aβ$_{1-42}$/Aβ$_{pE3-42}$) 50 mM NaCl + 50 mM Na,K-phosphate (pD 7.2) (C) and at 10 mM Na,K-phosphate buffers (pD 7.2) (D).

We were also interested in how Aβ$_{pE3-42}$ affects Aβ$_{1-42}$ peptide fibrillization kinetics. Specifically, the role that ionic strength plays in Aβ mixture fibrillization. For this purpose we incubated peptide samples with ThT which has been shown to fluoresce in the visible range when associated to amyloid fibrils.[93] Experiments were performed at 37°C while gently stirring. Additionally, two different salt concentrations were used to determine the effect of ionic strength on peptide fibrillization kinetics. Experiments were done in aqueous buffer containing 10 mM phosphate at pH 7.2 and at 50 mM Na,K-phosphate and 50 mM NaCl at pH 7.2.

Fibrilization kinetics of $A\beta_{1-42}$ under two different ionic strength conditions produced varying results. This suggests a determining role played by salt in Aβ interactions. A double exponential curve fit was used to determine the nucleation and elongation events of $A\beta_{1-42}$ **(fig 10. black lines)**. In 10 mM phosphate buffer at pH 7.2 the time constants are $\tau_0 = 21$ hours and $\tau_1 = 2.27$ hours. The nucleation event is described by $\tau_0$, which in turn, corresponds to a slower rate compared to $\tau_1$. The formation of the nucleus is thought to be formed after several thermodynamically unfavorable steps and thus is the slow step in the fibrillization process.

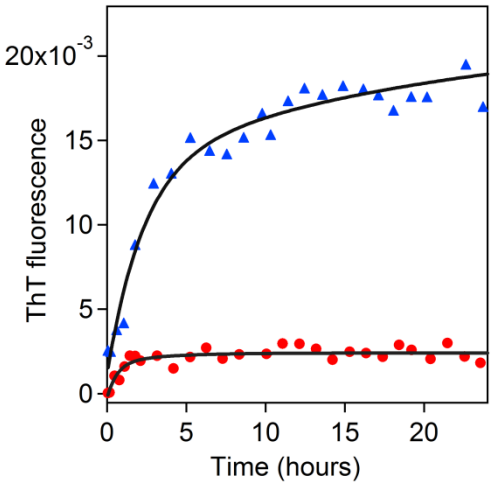


Figure 10. ThT fluorescence of $A\beta_{1-42}$ in 50 mM Na,K phosphate + 50 mM NaCl (red circles) and in 10 mM Na,K phosphate (blue triangles) buffers at pH 7.2 and at 37°C. Black lines are double exponential curve fittings of data points.

In high ionic strength conditions ThT signal reaches a maximum at ~ 2.3 hours. The respective time constants are $\tau_0 = 3.13$ hours and $\tau_1 = 0.63$ hours. Under high ionic strength conditions both nucleation and elongation time constants are lower than when there is less salt. This suggests that $A\beta_{1-42}$ forms antiparallel β-sheets which are destabilized by higher ionic strength. There is also a significant difference in maximum intensity of ThT fluorescence. At higher salt concentrations there could be less fibrils. This notion can be

related to the low rate constants when compared to lower ionic strength. Molecular dynamics simulations have suggested that ThT binds to fibril side channels.[95, 118] Others have identified at least two binding modes for ThT on amyloid fibrils.[119] This implies that subtle differences in binding mode could be related to aggregate secondary structure and can cause variability in ThT signal intensity.

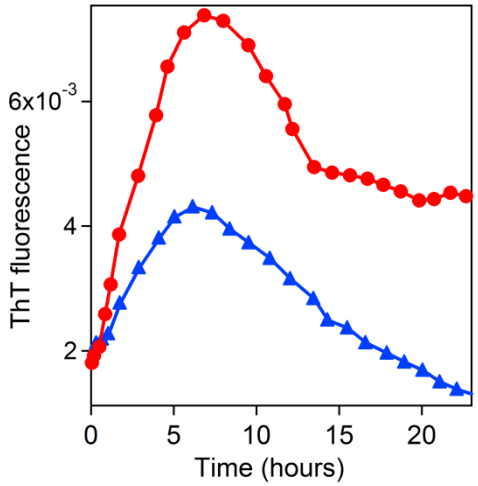


Figure 11. ThT fluorescence of $A\beta_{pE3-42}$ in 50 Na,K mM phosphate and 50 mM NaCl (red circles) and in 10 Na,K mM phosphate (blue triangles) buffers at pH 7.2 and 37°C.

Fibrillization kinetic experiments of $A\beta_{pE3-42}$ are shown in **(fig. 11)**. In this case higher ionic strength yields a higher ThT signal. This suggests that contrary to the unmodified peptide, $A\beta_{pE3-42}$ probably forms in register parallel β-sheets, which are stabilized by the salt's screening effect. Higher salt concentration screens the aligned residues with the same charge and thus stabilizes the secondary structure.

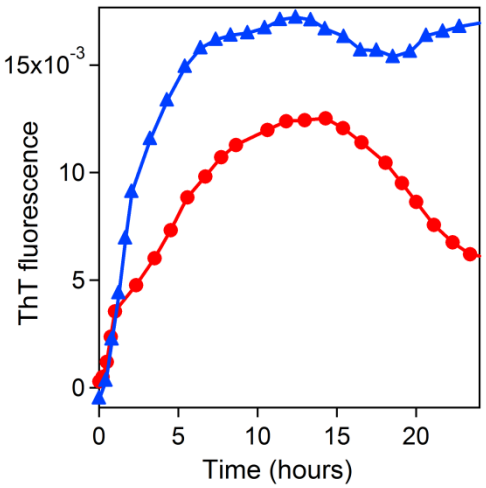


Figure 12. ThT fluorescence of the 1:1 combination in 50 mM Na,K phosphate and 50 mM NaCl (red circles) and in 10 mM phosphate (blue triangles) buffers at pH 7.2 and 37$^{o}$C.

At equimolar concentrations, low ionic strength conditions promote fibrillization when compared to high salt concentrations **(Fig. 12)**. Even though lower salt conditions promote faster kinetics the maximum signal is at ~12.5 hours for both conditions. Interestingly, at higher ionic strength there is a decrease in ThT fluorescence while the sample in low salt shows no decreasing trend.

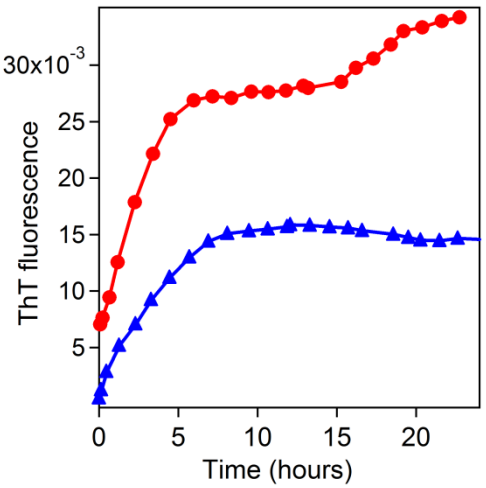


Figure 13. ThT fluorescence of the 9:1 combination in 50 mM Na,K phosphate + 50 mM NaCl (red circles) and in 10 mM phosphate (blue triangles) buffers at pH 7.2.

At a 9:1 $A\beta_{1\text{-}42}/A\beta_{pE3\text{-}42}$ **(Fig. 13)** combination there is no decrease in the ThT intensity as observed for $A\beta_{1\text{-}42}$ **(Fig. 10)**. Importantly, high ionic strength conditions result in higher ThT signal, as is the case for $A\beta_{pE3\text{-}42}$. The amount of the pyroglutamylated species is 10% of the total peptide, indicating that this behavior cannot be ascribed to an overwhelming $A\beta_{pE3\text{-}42}$ concentration. This data show the prion like effect that $A\beta_{pE3\text{-}42}$ has on Aβ aggregation. At low salt conditions, ThT fluorescence remains stagnant from ~7 to ~17 hours. Possible explanations for this are two-fold. First, the rates of fibril extension and shrinkage are the same, thus resulting in a zero net effect. Second, fibrils remain in a stagnant state where elongation does not occur.

The fibril shrinkage suggested by ThT assay seen in the 1:1 combination and in the $A\beta_{pE3\text{-}42}$, has been monitored by other groups.[28, 120] The decrease in ThT signal after reaching a maximum has been suggested to be caused by the aggregation of additional protein on labeled sites and thus blocking the ThT molecule. This theory is inadequate and poorly explains the observed effect. If this was the case then an explanation of why this only

happens in some cases is required. Other have suggested that the elongated fibrils precipitate and escape the window being measured.[120] This also lacks an explanation on why this would only happen occasionally. There have been reports of fibril disassembly when there is a lack of monomers.[28] These experiments showed that fibrils elongation and shrinkage are directly and inversely related to free monomer concentration, respectively. The constant ThT signal observed in the 9:1 and $A\beta_{1-42}$ samples have been previously described by following fibrillization with AFM.[121] Elongation occurs in small bursts when the fibril end is unblocked and stops when it is blocked; fibrils grow on both ends but at different rates.[121]

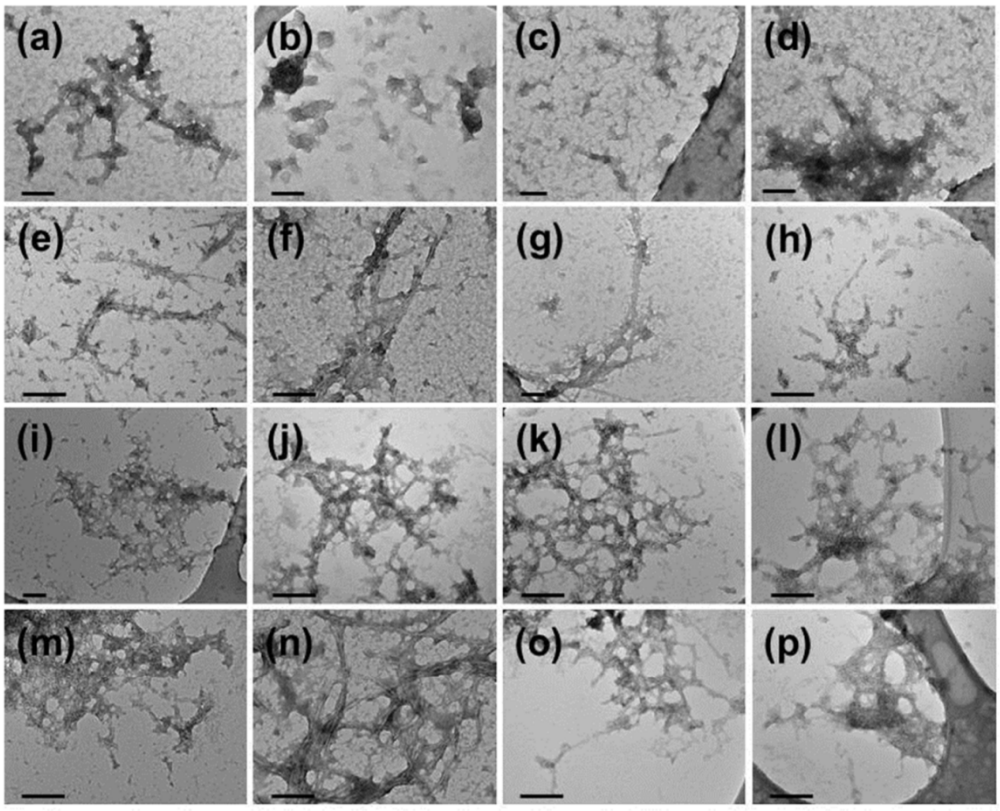


Figure 14. TEM images of $A\beta_{1-42}$ (a, e, i, m), $A\beta_{pE3-42}$ (b, f, j, n), $A\beta_{pE3-42}/A\beta_{1-42}$ = 1:9 (c, g, k, o), and $A\beta_{pE3-42}/A\beta_{1-42}$ = 1:1 (d, h, l, p) incubated in aqueous buffer of 50 mM NaCl and 50 mM Na,K-phosphate (pH 7.2) for 2 h (a-d), 4 h (e-h), 12 h (i-l), and 24 h (m-p) at 37$^{o}$C with constant stirring. The horizontal bar in each panel equals 100 nm.

A high degree of variation in fibrillization kinetics and ThT fluorescent intensities suggest different fibril morphologies. To study the morphology of Aβ fibrils and aggregates, we employed TEM and AFM. TEM measurements taken at 2,4,12 and 24 hours of incubation show that Aβ peptides, their 9:1 and 1:1 molar combinations fibrillize under 50 mM phosphate and 50 mM NaCl at pH 7.2 **(fig. 14)**. At 2 hours of incubation fibrils are observed for $A\beta_{1\text{-}42}$ while $A\beta_{pE\ 3\text{-}42}$ forms small non-fibrillar aggregates **(fig. 14 a,b)**. Meanwhile, the 9:1 and 1:1 molar combinations show fibrillar structures as early as 2 hours **(fig. 14 c,d)**. After four hours of incubation all samples show fibrils **(fig.14 e-h)**. Additionally, At 24 hours all samples show dense entangled fibrils **(fig. 14 m-p)**. Interestingly, $A\beta_{pE3\text{-}42}$ shows bundled fibrils.

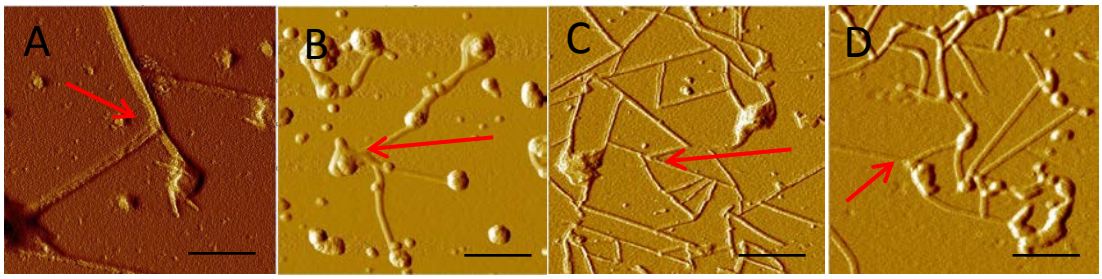


Figure 15. AFM images of $A\beta_{1\text{-}42}$ (A), $A\beta_{pE3\text{-}42}$ (B), $A\beta_{1\text{-}42}/A\beta_{pE3\text{-}42}$ (9:1) (C), and 1:1 (D) combinations, incubated in aqueous buffer of 50 mM NaCl and 50 mM Na,K phosphate (pH 7.2) at 37°C with constant stirring. Black lines correspond to 200 nm. Red lines show second nucleation sites.

Further morphological studies were performed by employing AFM on Aβ peptide samples that were incubated for 24 hours. Fibril preparation was done using the same procedure as for the TEM experiments (see above). In agreement with TEM images, AFM images show that $A\beta_{1-42}$ forms denser aggregates while $A\beta_{pE3\text{-}42}$ shows more flexible and polymorphic fibrillar structures (**fig. 15 a,b**). Both peptides by themselves show fibrillar structures which have an average diameter of approximately 45 nm. When combined at a 9:1

ratio the average diameter decreases to approximately 38 nm (**Fig. 15 c**) Fibrils prepared from equimolar concentrations show an increase in size to approximately 55 nm when compared to the peptides by themselves.

Second nucleation sites are defined as extending fibrils branching out of previously formed fibrils and have been recently described.[102] Our peptides samples show several second nucleation sites and examples have been labeled with red arrows. Also, fibrils extend from nucleation sites, which are globular aggregates present in all of the samples. As shown by TEM and AFM, pyroglutamated Aβ shows unique fibrillar features and also has a significant effect on unmodified Aβ aggregate formation.

Our results give mechanistic insight into previously established postulates. In mixture $A\beta_{1\text{-}42}$ and $A\beta_{pE3\text{-}42}$ show strong intermolecular interactions in buffer conditions. At equimolar concentrations $A\beta_{pE3\text{-}42}$ has increased turn component when compared to $A\beta_{pE3\text{-}42}$ by itself. Varying salt concentrations affect $A\beta_{1\text{-}42}$ secondary structure. At increased salt concentrations the turn to sheet ratio is increased. Additionally, the tertiary structure of a 1:1 combination is salt dependent. High salt promotes an open tertiary structure, while low salt promotes a tight, compact structure.

Differences in secondary and tertiary structure shed light on disagreements seen in previous published fibrillization data. Low salt conditions promote $A\beta_{1\text{-}42}$ fibrillization while inhibiting fibrillization of $A\beta_{pE3\text{-}42.}$ Importantly, at 10% $A\beta_{pE3\text{-}42}$, the fibrillization trend follows that of the pyroglutamylated peptide by itself. This cannot be accredited to a majority of $A\beta_{pE3\text{-}42}$ content. Our data suggest that $A\beta_{pE3\text{-}42}$ is able to transmit structural features to $A\beta_{1\text{-}42}$. Subsequently, $A\beta_{1\text{-}42}$ is able to infect other unmodified Aβ.

# CHAPTER FIVE: CONCLUSIONS

Our work aimed at the elucidation of the effect of $A\beta_{pE3-42}$ on $A\beta_{1-42}$ structure, fibrillization kinetics and final fibril morphology. It has been previously established that Aβ peptides are mostly α-helical in fluorinated alcohols such as HFIP. Interestingly, our data show that retention of the helical conformation following desiccation is dependent on total peptide concentration and humidity content. At 200 μM $A\beta_{1-42}$ and $A\beta_{pE3-42}$ show a prominent β-sheet component when dried. Conversely, at 50 μM $A\beta_{1-42}$, $A\beta_{pE3-42}$, their 9:1 and 1:1 combinations show mostly α-helical structure after desiccation. These results carry an important implication. Many experiments that follow aggregation behavior claim a seedless and nucleus free starting point. Nevertheless, this may not be the case even when using methods that have been shown to break aggregates and promote monomeric form. For such experiments care should be taken and rigorous verification should be employed.

Our data suggest that initial concentrations of stocks might affect peptide structure in experiments and thus result in incongruences. This is especially important since oligomeric species and fibrils have been shown to be capable of forming through different pathways; presence of oligomer does not imply mandatory fibril formation.[122]

Addition of bulk $D_2O$ buffer promotes β-sheet structure in both $A\beta_{pE3-42}$ and $A\beta_{1-42}$. The increased presence of α-helical structure in $A\beta_{pE3-42}$ suggests that this species does not fibrillize from the same starting point as $A\beta_{1-42}$. Additionally, it helps explain the significant difference in toxicity when compared to $A\beta_{1-42}$.

Isotope edited FTIR permitted us to identify strong interactions between the peptides. Our data also show that mixed peptides samples in buffer show different secondary structures when compared to their algebraic combination. When combined at equimolar concentrations the turn to sheet ratio decreases significantly for $A\beta_{pE3-42}$.

Our FTIR data show that the transition to β-sheet after buffer addition occurs in an undetectable amount of time. Interest in the transitional states following interaction of monomers has increased since focus on soluble oligomeric species was established. To determine intermediate structures between the dried state and aqueous of AD relevant Aβ mixtures, we exposed the 9:1 and 1:1 combinations to nominal environmental humidity. The addition of nominal environmental moisture is sufficient to induce gradual conformational changes on Aβ peptides. $A\beta_{pE3-42}$ at 10% total peptide concentration causes an inhibition of β-sheet formation by the $A\beta_{1-42}$. Strikingly, At equimolar concentrations the pyroglutamylated peptide was able to reverse cross β-sheet formation. Our data show for the first time a detailed prion effect of $A\beta_{pE3-42}$ on $A\beta_{1-42}$ secondary structure. This has given some structural insight into previous reports that show for example, that at low $A\beta_{pE3-42}$ %, Aβ mixtures are most toxic. Few examples exist of proteins that have been shown to be structurally affected by humidity.[123] This implies that careful preparation in controlled environments is essential for Aβ samples before experiments This potentially applies to other fibril forming peptides such as α-synuclein causatively linked to Parkinson's disease.[124]

Addition of $D_2O$ saturated nitrogen gas showed dynamic changes of Aβ peptides at a 1:1 combination. Initially, both peptides show prominent α-helical conformation; $Aβ_{1-42}$ transitions to β-sheet upon hydration. Interestingly, hydration promotes a strong turn region belonging to the pyrogltamylated peptide. Upon removal of windows from sample chamber, $Aβ_{pE3-42}$ transitions from a β-sheet to a more unordered/helical state. Our data show that a higher degree of hydration does not imply a linear trend from α-helical to β-sheet as was hypothesized.

By CD we determined that upon addition of bulk aqueous buffer all samples undergo a structural transition towards β-sheet structures, albeit not with the same intensity. The 9:1 combination and $Aβ_{1-42}$ showed strong β-sheet signal while $Aβ_{pE3-42}$ and the 1:1 combination showed a weaker signal. This corresponds to higher degree of β-sheets as intensity increases.

Fibrillization studies by ThT fluorescence show that ionic strength plays a determining role on peptide aggregation. $Aβ_{1-42}$ shows higher ThT signal at lower salt concentrations. Conversely, $Aβ_{pE3-42}$ has increased fibrillization at higher salt concentrations. These data suggest that in the case for $Aβ_{pE3-42}$, the peptide forms parallel β-sheets, where the salt helps screen like charges of interacting residues. Interestingly, at a 9:1 combination the trend followed is similar to the $Aβ_{pE3-42}$. At equimolar ratio the trend followed corresponds to the $Aβ_{1-42}$ peptide. This shows that the effect of $Aβ_{pE3-42}$ on $Aβ_{1-42}$ does not follow superposition principles. The effect of salt and Aβ ratio led us to hypothesize that significant secondary structure differences exist in Aβ fibril seeds. As determined by FTIR at high ionic strength $Aβ_{1-42}$ shows increased turn to sheet ratio, when compared to low salt conditions. Most notably, at high ionic strength, $Aβ_{pE3-42}$ shows helical components not significantly present at low salt. These data show that $Aβ_{pE3-42}$ is able to produce positive ThT signal while

not being in pure cross β-sheet structure. Thus expanding structural conformations ThT can bind to.

When combined at 9:1 our data show a larger turn to sheet ratio than at lower salt. Interestingly, higher turn to sheet ratio is not sufficient to promote ThT signal. Since $A\beta_{1\text{-}42}$ fibrillizes more readily at lower ionic strength where less turn component is present. Further structural studies are necessary to determine spatial resolution of Aβ peptides and determine underlying factors that affect Aβ secondary structure and aggregation.

By employing TEM we identified distinct fibrillization pathways. At 2 hours of incubation $A\beta_{1\text{-}42}$ shows fibril formation while $A\beta_{pE3\text{-}42}$ shows small irregular shaped aggregates. The 9:1 and 1:1 combinations contain pre-fibrillar structures. After 24 hours all samples show fibrillar aggregates. Our data show that distinct fibrillization pathways are followed by Aβ and their combinations. These data help shed light on possible toxic species. For example, low molar content of $A\beta_{pE3\text{-}42}$ has been shown to be hypertoxic to cultured neurons. Additionally, oligomers and not fibrils are currently thought to be most toxic. Our TEM data for the 9:1 combination show lack of mature fibrils after 4 hours of incubation. These data suggest that small oligomers cause neuronal death and that possibly fibrils act as a rescue mechanism and are not the main toxic entities.

AFM data further elucidated fibril morphology. At a 1:1 combination the fibrils have fibril morphology that is intermediate between $A\beta_{1\text{-}42}$ and $A\beta_{pE3\text{-}42}$. Nucleation and second nucleation sites can be observed, giving indication of fibril initial elongation sites and branching sites. Our data show that $A\beta_{pE3\text{-}42}$ affects $A\beta_{1\text{-}42}$ at a molecular and ultrastructural level.

Non fibrillar oligomeric species are thought to be the toxic entities in AD. Strikingly, our studies confirm that not only does ionic strength affect Aβ secondary structure but also fibril stability. At equimolar concentrations, physiologically relevant ionic strength ThT studies, show that fibrils disassemble before 24 hours of incubation, while ThT fluorescence does not decrease at low salt. Further toxicity studies are needed to determine if this loss in fibrillar structure has a positive correlation with increased “pathological conformations” in AD.

# LIST OF REFERENCES


1. Querfurth, H. W., and LaFerla, F. M. (2010) Mechanisms of disease alzheimer's disease, *New England Journal of Medicine 362*, 329-344.

2. Hardy, J. A., and Higgins, G. A. (1992) Alzheimers-disease - the amyloid cascade hypothesis, *Science 256*, 184-185.

3. Pike, C. J., Burdick, D., Walencewicz, A. J., Glabe, C. G., and Cotman, C. W. (1993) Neurodegeneration induced by beta-amyloid peptides invitro - the role of peptide assembly state, *Journal of Neuroscience 13*, 1676-1687.

4. Dahlgren, K. N., Manelli, A. M., Stine, W. B., Baker, L. K., Krafft, G. A., and LaDu, M. J. (2002) Oligomeric and fibrillar species of amyloid-beta peptides differentially affect neuronal viability, *Journal of Biological Chemistry 277*, 32046-32053.

5. Kirkitadze, M. D., Bitan, G., and Teplow, D. B. (2002) Paradigm shifts in Alzheimer's disease and other neuro degenerative disorders: The emerging role of oligomeric assemblies, *Journal of Neuroscience Research 69*, 567-577.

6. Klein, W. L., Stine, W. B., and Teplow, D. B. (2004) Small assemblies of unmodified amyloid beta-protein are the proximate neurotoxin in Alzheimer's disease, *Neurobiology of Aging 25*, 569-580.

7. Bitan, G., Fradinger, E. A., Spring, S. M., and Teplow, D. B. (2005) Neurotoxic protein oligomers - what you see is not always what you get, *Amyloid-Journal of Protein Folding Disorders 12*, 88-95.

8. Resende, R., Ferreiro, E., Pereira, C., and De Oliveira, C. R. (2008) Neurotoxic effect of oligomeric and fibrillar species of amyloid-beta peptide 1-42: Involvement of endoplasmic reticulum calcium release in oligomer-induced cell death, *Neuroscience 155*, 725-737.

9. Bernstein, S. L., Dupuis, N. F., Lazo, N. D., Wyttenbach, T., Condron, M. M., Bitan, G., Teplow, D. B., Shea, J. E., Ruotolo, B. T., Robinson, C. V., and Bowers, M. T. (2009) Amyloid-β protein oligomerization and the importance of tetramers and dodecamers in the aetiology of Alzheimer's disease, *Nat Chem 1*, 326-331.

10. Masters, C. L., and Selkoe, D. J. (2012) Biochemistry of Amyloid beta-Protein and Amyloid Deposits in Alzheimer Disease, *Cold Spring Harbor Perspectives in Medicine 2*.

11. Schilling, S., Lauber, T., Schaupp, M., Manhart, S., Scheel, E., Boehm, G., and Demuth, H.-U. (2006) On the seeding and oligomerization of pGlu-amyloid peptides (in vitro), *Biochemistry 45*, 12393-12399.

12. Schlenzig, D., Manhart, S., Cinar, Y., Kleinschmidt, M., Hause, G., Willbold, D., Funke, S. A., Schilling, S., and Demuth, H.-U. (2009) Pyroglutamate Formation

Influences Solubility and Amyloidogenicity of Amyloid Peptides, *Biochemistry 48*, 7072-7078.

13. Schlenzig, D., Roenicke, R., Cynis, H., Ludwig, H.-H., Scheel, E., Reymann, K., Saido, T., Hause, G., Schilling, S., and Demuth, H.-U. (2012) N-Terminal pyroglutamate formation of A beta 38 and A beta 40 enforces oligomer formation and potency to disrupt hippocampal long-term potentiation, *Journal of Neurochemistry 121*, 774-784.

14. Jawhar, S., Wirths, O., and Bayer, T. A. (2011) Pyroglutamate Amyloid-beta (A beta): A Hatchet Man in Alzheimer Disease, *Journal of Biological Chemistry 286*, 38825-38832.

15. Nussbaum, J. M., Schilling, S., Cynis, H., Silva, A., Swanson, E., Wangsanut, T., Tayler, K., Wiltgen, B., Hatami, A., Roenicke, R., Reymann, K., Hutter-Paier, B., Alexandru, A., Jagla, W., Graubner, S., Glabe, C. G., Demuth, H.-U., and Bloom, G. S. (2012) Prion-like behaviour and tau-dependent cytotoxicity of pyroglutamylated amyloid-beta, *Nature 485*, 651-655.

16. Ramirez-Bermudez, J. (2012) Alzheimer's Disease: Critical Notes on the History of a Medical Concept, *Archives of Medical Research 43*, 595-599.

17. Maurer, K., Volk, S., and Gerbaldo, H. (1997) Auguste D and Alzheimer's disease, *Lancet 349*, 1546-1549.

18. Glenner, G. G., and Wong, C. W. (1984) Alzheimers-disease - initial report of the purification and characterization of a novel cerebrovascular amyloid protein, *Biochemical and Biophysical Research Communications 120*, 885-890.

19. McLean, C. A., Cherny, R. A., Fraser, F. W., Fuller, S. J., Smith, M. J., Beyreuther, K., Bush, A. I., and Masters, C. L. (1999) Soluble pool of A beta amyloid as a determinant of severity of neurodegeneration in Alzheimer's disease, *Annals of Neurology 46*, 860-866.

20. Pimplikar, S. W. (2009) Reassessing the amyloid cascade hypothesis of Alzheimer's disease, *International Journal of Biochemistry & Cell Biology 41*, 1261-1268.

21. Haass, C., and Selkoe, D. J. (2007) Soluble protein oligomers in neurodegeneration: lessons from the Alzheimer's amyloid beta-peptide, *Nature Reviews Molecular Cell Biology 8*, 101-112.

22. Zhang, X., and Song, W. (2013) The role of APP and BACE1 trafficking in APP processing and amyloid-beta generation, *Alzheimers Research & Therapy 5*.

23. Mehta, P. D., Pirttila, T., Mehta, S. P., Sersen, E. A., Aisen, P. S., and Wisniewski, H. M. (2000) Plasma and cerebrospinal fluid levels of amyloid beta proteins 1-40 and 1-42 in Alzheimer disease, *Archives of Neurology 57*, 100-105.

24. Masters, C. L., Simms, G., Weinman, N. A., Multhaup, G., McDonald, B. L., and Beyreuther, K. (1985) Amyloid plaque core protein in alzheimer-disease and down

syndrome, *Proceedings of the National Academy of Sciences of the United States of America 82*, 4245-4249.

25. Russo, C., Violani, E., Salis, S., Venezia, V., Dolcini, V., Damonte, G., Benatti, U., D'Arrigo, C., Patrone, E., Carlo, P., and Schettini, G. (2002) Pyroglutamate-modified amyloid beta-peptides - A beta N3(pE)-strongly affect cultured neuron and astrocyte survival, *Journal of Neurochemistry 82*, 1480-1489.

26. Antzutkin, O. N., Leapman, R. D., Balbach, J. J., and Tycko, R. (2002) Supramolecular structural constraints on Alzheimer's beta-amyloid fibrils from electron microscopy and solid-state nuclear magnetic resonance, *Biochemistry 41*, 15436-15450.

27. Petkova, A. T., Yau, W. M., and Tycko, R. (2006) Experimental constraints on quaternary structure in Alzheimer's beta-amyloid fibrils, *Biochemistry 45*, 498-512.

28. Qiang, W., Kelley, K., and Tycko, R. (2013) Polymorph-Specific Kinetics and Thermodynamics of beta-Amyloid Fibril Growth, *Journal of the American Chemical Society 135*, 6860-6871.

29. He, W. L., and Barrow, C. J. (1999) The A beta 3-pyroglutamyl and 11-pyroglutamyl peptides found in senile plaque have greater beta-sheet forming and aggregation propensities in vitro than full-length A beta, *Biochemistry 38*, 10871-10877.

30. D'Arrigo, C., Tabaton, M., and Perico, A. (2009) N-Terminal Truncated Pyroglutamyl beta Amyloid Peptide A beta py3-42 Shows a Faster Aggregation Kinetics than the Full-Length A beta 1-42, *Biopolymers 91*, 861-873.

31. Sanders, H. M., Lust, R., and Teller, J. K. (2009) Amyloid-beta peptide A beta p3-42 affects early aggregation of full-length A beta 1-42, *Peptides 30*, 849-854.

32. Harigaya, Y., Saido, T. C., Eckman, C. B., Prada, C. M., Shoji, M., and Younkin, S. G. (2000) Amyloid beta protein starting pyroglutamate at position 3 is a major component of the amyloid deposits in the Alzheimer's disease brain, *Biochemical and Biophysical Research Communications 276*, 422-427.

33. Mori, H., Takio, K., Ogawara, M., and Selkoe, D. (1992) Mass-spectrometry of purified amyloid-beta protein in alzheimers-disease, *Journal of Biological Chemistry 267*, 17082-17086.

34. Piccini, A., Russo, C., Gliozzi, A., Relini, A., Vitali, A., Borghi, R., Giliberto, L., Armirotti, A., D'Arrigo, C., Bachi, A., Cattaneo, A., Canale, C., Torrassa, S., Saido, T. C., Markesbery, W., Gambetti, P., and Tabaton, M. (2005) beta-amyloid is different in normal aging and in Alzheimer disease, *J Biol Chem 280*, 34186-34192.

35. Ahmadi, S., and Wade-Martins, R. (2014) Familial Alzheimer's disease coding mutations reduce Presenilin-1 expression in a novel genomic locus reporter model, *Neurobiology of Aging 35*.

36. Sherrington, R., Rogaev, E. I., Liang, Y., Rogaeva, E. A., Levesque, G., Ikeda, M., Chi, H., Lin, C., Li, G., Holman, K., Tsuda, T., Mar, L., Foncin, J. F., Bruni, A. C., Montesi, M. P., Sorbi, S., Rainero, I., Pinessi, L., Nee, L., Chumakov, I., Pollen, D., Brookes, A., Sanseau, P., Polinsky, R. J., Wasco, W., Dasilva, H. A. R., Haines, J. L., Pericakvance, M. A., Tanzi, R. E., Roses, A. D., Fraser, P. E., Rommens, J. M., and Stgeorgehyslop, P. H. (1995) Cloning of a gene bearing missense mutations in early-onset familial alzheimers-disease, *Nature 375*, 754-760.

37. LevyLahad, E., Poorkaj, P., Wang, K., Fu, Y. H., Oshima, J., Mulligan, J., and Schellenberg, G. D. (1996) Genomic structure and expression of STM2, the chromosome 1 familial Alzheimer disease gene, *Genomics 34*, 198-204.

38. Goate, A. (2006) Segregation of a missense mutation in the amyloid beta-protein precursor gene with familial Alzheimer's disease, *Alzheimer's Disease: a Century of Scientific and Clinical Research*, 341-347.

39. Citron, M., Oltersdorf, T., Haass, C., McConlogue, L., Hung, A. Y., Seubert, P., Vigopelfrey, C., Lieberburg, I., and Selkoe, D. J. (1992) Mutation of the beta-amyloid precursor protein in familial alzheimers-disease increases beta-protein production, *Nature 360*, 672-674.

40. Pooler, A. M., Noble, W., and Hanger, D. P. (2014) A role for tau at the synapse in Alzheimer's disease pathogenesis, *Neuropharmacology 76 Pt A*, 1-8.

41. Zempel, H., Thies, E., Mandelkow, E., and Mandelkow, E.-M. (2010) A beta Oligomers Cause Localized Ca2+ Elevation, Missorting of Endogenous Tau into Dendrites, Tau Phosphorylation, and Destruction of Microtubules and Spines, *Journal of Neuroscience 30*, 11938-11950.

42. Davis, D. G., Schmitt, F. A., Wekstein, D. R., and Markesbery, W. R. (1999) Alzheimer neuropathologic alterations in aged cognitively normal subjects, *Journal of Neuropathology and Experimental Neurology 58*, 376-388.

43. Lesne, S. E., Sherman, M. A., Grant, M., Kuskowski, M., Schneider, J. A., Bennett, D. A., and Ashe, K. H. (2013) Brain amyloid-beta oligomers in ageing and Alzheimer's disease, *Brain 136*, 1383-1398.

44. Wu, W.-h., Liu, Q., Sun, X., Yu, J.-s., Zhao, D.-s., Yu, Y.-p., Luo, J.-j., Hu, J., Yu, Z.-w., Zhao, Y.-f., and Li, Y.-m. (2013) Fibrillar seeds alleviate amyloid-beta cytotoxicity by omitting formation of higher-molecular-weight oligomers, *Biochemical and Biophysical Research Communications 439*, 321-326.

45. Giuffrida, M. L., Caraci, F., Pignataro, B., Cataldo, S., De Bona, P., Bruno, V., Molinaro, G., Pappalardo, G., Messina, A., Palmigiano, A., Garozzo, D., Nicoletti, F., Rizzarelli, E., and Copani, A. (2009) beta-Amyloid Monomers Are Neuroprotective, *Journal of Neuroscience 29*, 10582-10587.

46. Shankar, G. M., Li, S., Mehta, T. H., Garcia-Munoz, A., Shepardson, N. E., Smith, I., Brett, F. M., Farrell, M. A., Rowan, M. J., Lemere, C. A., Regan, C. M., Walsh, D. M., Sabatini, B. L., and Selkoe, D. J. (2008) Amyloid-beta protein dimers isolated

directly from Alzheimer's brains impair synaptic plasticity and memory, *Nature Medicine 14*, 837-842.

47. Townsend, M., Shankar, G. M., Mehta, T., Walsh, D. M., and Selkoe, D. J. (2006) Effects of secreted oligomers of amyloid beta-protein on hippocampal synaptic plasticity: a potent role for trimers, *Journal of Physiology-London 572*, 477-492.

48. Bernstein, S. L., Dupuis, N. F., Lazo, N. D., Wyttenbach, T., Condron, M. M., Bitan, G., Teplow, D. B., Shea, J.-E., Ruotolo, B. T., Robinson, C. V., and Bowers, M. T. (2009) Amyloid-beta protein oligomerization and the importance of tetramers and dodecamers in the aetiology of Alzheimer's disease, *Nature Chemistry 1*, 326-331.

49. Lesne, S., Koh, M. T., Kotilinek, L., Kayed, R., Glabe, C. G., Yang, A., Gallagher, M., and Ashe, K. H. (2006) A specific amyloid-beta protein assembly in the brain impairs memory, *Nature 440*, 352-357.

50. Ferreiro, E., Oliveira, C. R., and Pereira, C. M. F. (2008) The release of calcium from the endoplasmic reticulum induced by amyloid-beta and prion peptides activates the mitochondrial apoptotic pathway, *Neurobiology of Disease 30*, 331-342.

51. Kim, T., Vidal, G. S., Djurisic, M., William, C. M., Birnbaum, M. E., Garcia, K. C., Hyman, B. T., and Shatz, C. J. (2013) Human LilrB2 Is a beta-Amyloid Receptor and Its Murine Homolog PirB Regulates Synaptic Plasticity in an Alzheimer's Model, *Science 341*, 1399-1404.

52. Isaacs, A. M., Senn, D. B., Yuan, M., Shine, J. P., and Yankner, B. A. (2006) Acceleration of amyloid beta-peptide aggregation by physiological concentrations of calcium, *Journal of Biological Chemistry 281*, 27916-27923.

53. Hou, L.-N., Xu, J.-R., Zhao, Q.-N., Gao, X.-L., Cui, Y.-Y., Xu, J., Wang, H., and Chen, H.-Z. (2014) A New Motif in the N-Terminal of Acetylcholinesterase Triggers Amyloid-beta Aggregation and Deposition, *Cns Neuroscience & Therapeutics 20*, 59-66.

54. Benilova, I., Karran, E., and De Strooper, B. (2012) The toxic A beta oligomer and Alzheimer's disease: an emperor in need of clothes, *Nature Neuroscience 15*, 349-357.

55. Zandomeneghi, G., Krebs, M. R., McCammon, M. G., and Fändrich, M. (2004) FTIR reveals structural differences between native beta-sheet proteins and amyloid fibrils, *Protein Sci 13*, 3314-3321.

56. Petkova, A. T., Ishii, Y., Balbach, J. J., Antzutkin, O. N., Leapman, R. D., Delaglio, F., and Tycko, R. (2002) A structural model for Alzheimer's beta-amyloid fibrils based on experimental constraints from solid state NMR, *Proceedings of the National Academy of Sciences of the United States of America 99*, 16742-16747.

57. Chiti, F., and Dobson, C. M. (2006) Protein misfolding, functional amyloid, and human disease, *Annual Review of Biochemistry 75*, 333-366.

58. Kar, K., Hoop, C. L., Drombosky, K. W., Baker, M. A., Kodali, R., Arduini, I., van der Wel, P. C. A., Horne, W. S., and Wetzelt, R. (2013) beta-Hairpin-Mediated Nucleation of Polyglutamine Amyloid Formation, *Journal of Molecular Biology 425*, 1183-1197.

59. Cheng, H., Wang, L., and Wang, C.-c. (2010) Domain a' of protein disulfide isomerase plays key role in inhibiting alpha-synuclein fibril formation, *Cell Stress & Chaperones 15*, 415-421.

60. Blancas-Mejia, L. M., Tischer, A., Thompson, J. R., Tai, J., Wang, L., Auton, M., and Ramirez-Alvarado, M. (2014) Kinetic Control in Protein Folding for Light Chain Amyloidosis and the Differential Effects of Somatic Mutations, *Journal of Molecular Biology 426*, 347-361.

61. Cao, P., Tu, L.-H., Abedini, A., Levsh, O., Akter, R., Patsalo, V., Schmidt, A. M., and Raleigh, D. P. (2012) Sensitivity of Amyloid Formation by Human Islet Amyloid Polypeptide to Mutations at Residue 20, *Journal of Molecular Biology 421*, 282-295.

62. Wahlster, L., Arimon, M., Nasser-Ghodsi, N., Post, K. L., Serrano-Pozo, A., Uemura, K., and Berezovska, O. (2013) Presenilin-1 adopts pathogenic conformation in normal aging and in sporadic Alzheimer's disease, *Acta Neuropathologica 125*, 187-199.

63. Hunter, S., Arendt, T., and Brayne, C. (2013) The Senescence Hypothesis of Disease Progression in Alzheimer Disease: an Integrated Matrix of Disease Pathways for FAD and SAD, *Molecular Neurobiology 48*, 556-570.

64. Bjorkhem, I., and Meaney, S. (2004) Brain cholesterol: Long secret life behind a barrier, *Arteriosclerosis Thrombosis and Vascular Biology 24*, 806-815.

65. Holtzman, D. M., Herz, J., and Bu, G. (2012) Apolipoprotein E and Apolipoprotein E Receptors: Normal Biology and Roles in Alzheimer Disease, *Cold Spring Harbor Perspectives in Biology 4*.

66. Beel, A. J., Sakakura, M., Barrett, P. J., and Sanders, C. R. (2010) Direct binding of cholesterol to the amyloid precursor protein: An important interaction in lipid-Alzheimer's disease relationships?, *Biochimica Et Biophysica Acta-Molecular and Cell Biology of Lipids 1801*, 975-982.

67. Pasinetti, G. M., Wang, J., Porter, S., and Ho, L. (2011) Caloric intake, dietary lifestyles, macronutrient composition, and alzheimer' disease dementia, *International journal of Alzheimer's disease 2011*, 806293-806293.

68. Koivisto, H., Takalo, M., Miettinen, P., Broersen, L. M., and Tanila, H. (2011) Special lipid-based diets alleviate cognitive deficits in the appswe/ps1de9 transgenic mouse model of alzheimer's disease independent of brain amyloid deposition, *European Journal of Neurology 18*, 78-78.

69. Morris, M. C., Evans, D. A., Bienias, J. L., Tangney, C. C., Bennett, D. A., Wilson, R. S., Aggarwal, N., and Schneider, J. (2003) Consumption of fish and n-3 fatty acids and risk of incident Alzheimer disease, *Archives of Neurology 60*, 940-946.

70. Mondragon-Rodriguez, S., Perry, G., Zhu, X., Moreira, P. I., Acevedo-Aquino, M. C., and Williams, S. (2013) Phosphorylation of Tau Protein as the Link between Oxidative Stress, Mitochondrial Dysfunction, and Connectivity Failure: Implications for Alzheimer's Disease, *Oxidative Medicine and Cellular Longevity*.

71. Patterson, K. R., Remmers, C., Fu, Y., Brooker, S., Kanaan, N. M., Vana, L., Ward, S., Reyes, J. F., Philibert, K., Glucksman, M. J., and Binder, L. I. (2011) Characterization of Prefibrillar Tau Oligomers in Vitro and in Alzheimer Disease, *Journal of Biological Chemistry 286*, 23063-23076.

72. Gregory, J. L., Prada, C. M., Fine, S. J., Garcia-Alloza, M., Betensky, R. A., Arbel-Ornath, M., Greenberg, S. M., Bacskai, B. J., and Frosch, M. P. (2012) Reducing Available Soluble beta-Amyloid Prevents Progression of Cerebral Amyloid Angiopathy in Transgenic Mice, *Journal of Neuropathology and Experimental Neurology 71*, 1009-1017.

73. Mattson, M. P., Cheng, B., Davis, D., Bryant, K., Lieberburg, I., and Rydel, R. E. (1992) Beta-amyloid peptides destabilize calcium homeostasis and render human cortical-neurons vulnerable to excitotoxicity, *Journal of Neuroscience 12*, 376-389.

74. Bezprozvanny, I., and Mattson, M. P. (2008) Neuronal calcium mishandling and the pathogenesis of Alzheimer's disease, *Trends in Neurosciences 31*, 454-463.

75. Green, K. N., and LaFerla, F. M. (2008) Linking calcium to A beta and Alzheimer's disease, *Neuron 59*, 190-194.

76. Arispe, N., Rojas, E., and Pollard, H. B. (1993) Alzheimer-disease amyloid beta-protein forms calcium channels in bilayer-membranes - blockade by tromethamine and aluminum, *Proceedings of the National Academy of Sciences of the United States of America 90*, 567-571.

77. Sepulveda, F. J., Fierro, H., Fernandez, E., Castillo, C., Peoples, R. W., Opazo, C., and Aguayo, L. G. (2014) Nature of the neurotoxic membrane actions of amyloid-beta on hippocampal neurons in Alzheimer's disease, *Neurobiology of Aging 35*, 472-481.

78. Yoshiike, Y., Kayed, R., Milton, S. C., Takashima, A., and Glabe, C. G. (2007) Pore-forming proteins share structural and functional homology with amyloid oligomers, *Neuromolecular Medicine 9*, 270-275.

79. Supnet, C., Grant, J., Kong, H., Westaway, D., and Mayne, M. (2006) Amyloid-beta-(1-42) increases ryanodine receptor-3 expression and function in neurons of TgCRND8 mice, *Journal of Biological Chemistry 281*, 38440-38447.

80. Fonseca, A. C., Ferreiro, E., Oliveira, C. R., Cardoso, S. M., and Pereira, C. F. (2013) Activation of the endoplasmic reticulum stress response by the amyloid-beta 1-40 peptide in brain endothelial cells, *Biochim Biophys Acta 1832*, 2191-2203.

81. Um, J. W., Kaufman, A. C., Kostylev, M., Heiss, J. K., Stagi, M., Takahashi, H., Kerrisk, M. E., Vortmeyer, A., Wisniewski, T., Koleske, A. J., Gunther, E. C., Nygaard, H. B., and Strittmatter, S. M. (2013) Metabotropic glutamate receptor 5 is a

coreceptor for Alzheimer abeta oligomer bound to cellular prion protein, *Neuron 79*, 887-902.

82. Simakova, O., and Arispe, N. J. (2007) The cell-selective neurotoxicity of the Alzheimer's A beta peptide is determined by surface phosphatidylserine and cytosolic ATP levels. Membrane binding is required for A beta toxicity, *Journal of Neuroscience 27*, 13719-13729.

83. Arispe, N., and Doh, M. (2002) Plasma membrane cholesterol controls the cytotoxicity of Alzheimer's disease A beta P (1-40) and (1-42) peptides, *Faseb Journal 16*, 1526-1536.

84. Pensalfini, A., Zampagni, M., Liguri, G., Becatti, M., Evangelisti, E., Fiorillo, C., Bagnoli, S., Cellini, E., Nacmias, B., Sorbi, S., and Cecchi, C. (2011) Membrane cholesterol enrichment prevents A beta-induced oxidative stress in Alzheimer's fibroblasts, *Neurobiology of Aging 32*, 210-222.

85. Di Paolo, G., and Kim, T.-W. (2011) Linking lipids to Alzheimer's disease: cholesterol and beyond, *Nature Reviews Neuroscience 12*, 284-296.

86. Fantini, J., Di Scala, C., Yahi, N., Troadec, J.-D., Sadelli, K., Chahinian, H., and Garmy, N. (2014) Bexarotene Blocks Calcium-Permeable Ion Channels Formed by Neurotoxic Alzheimer's beta-Amyloid Peptides, *Acs Chemical Neuroscience 5*, 216-224.

87. Zhu, X., Perry, G., Smith, M. A., and Wang, X. (2013) Abnormal Mitochondrial Dynamics in the Pathogenesis of Alzheimer's Disease, *Alzheimer's Disease: Advances for a New Century 3*, 253-262.

88. Garcia-Escudero, V., Martin-Maestro, P., Perry, G., and Avila, J. (2013) Deconstructing Mitochondrial Dysfunction in Alzheimer Disease, *Oxidative Medicine and Cellular Longevity*.

89. Manczak, M., Anekonda, T. S., Henson, E., Park, B. S., Quinn, J., and Reddy, P. H. (2006) Mitochondria are a direct site of A beta accumulation in Alzheimer's disease neurons: implications for free radical generation and oxidative damage in disease progression, *Human Molecular Genetics 15*, 1437-1449.

90. Christen, Y. (2000) Oxidative stress and Alzheimer disease, *American Journal of Clinical Nutrition 71*, 621S-629S.

91. Manczak, M., Calkins, M. J., and Reddy, P. H. (2011) Impaired mitochondrial dynamics and abnormal interaction of amyloid beta with mitochondrial protein Drp1 in neurons from patients with Alzheimer's disease: implications for neuronal damage, *Human Molecular Genetics 20*, 2495-2509.

92. Galante, D., Corsaro, A., Florio, T., Vella, S., Pagano, A., Sbrana, F., Vassalli, M., Perico, A., and D'Arrigo, C. (2012) Differential toxicity, conformation and morphology of typical initial aggregation states of A beta 1-42 and A beta py3-42 beta-amyloids, *International Journal of Biochemistry & Cell Biology 44*, 2085-2093.

93. Levine, H. (1993) Thioflavine-t interaction with synthetic alzheimers-disease beta-amyloid peptides - detection of amyloid aggregation in solution, *Protein Science 2*, 404-410.

94. Krebs, M. R. H., Bromley, E. H. C., and Donald, A. M. (2005) The binding of thioflavin-T to amyloid fibrils: localisation and implications, *Journal of Structural Biology 149*, 30-37.

95. Biancalana, M., and Koide, S. (2010) Molecular mechanism of Thioflavin-T binding to amyloid fibrils, *Biochimica Et Biophysica Acta-Proteins and Proteomics 1804*, 1405-1412.

96. Greenfield, N. J. (2006) Using circular dichroism spectra to estimate protein secondary structure, *Nature Protocols 1*, 2876-2890.

97. Tatulian, S. A. (2013) Structural characterization of membrane proteins and peptides by FTIR and ATR-FTIR spectroscopy, *Methods in molecular biology (Clifton, N.J.) 974*, 177-218.

98. Li, T. S. (2004) Investigation of protein-protein interactions by isotope-edited Fourier transformed infrared spectroscopy, *Spectroscopy-an International Journal 18*, 397-406.

99. Halverson, K. J., Sucholeiki, I., Ashburn, T. T., and Lansbury, P. T. (1991) Location of beta-sheet-forming sequences in amyloid proteins by ftir, *Journal of the American Chemical Society 113*, 6701-6703.

100. Nilsson, M. R. (2004) Techniques to study amyloid fibril formation in vitro, *Methods 34*, 151-160.

101. Ahmed, M., Davis, J., Aucoin, D., Sato, T., Ahuja, S., Aimoto, S., Elliott, J. I., Van Nostrand, W. E., and Smith, S. O. (2010) Structural conversion of neurotoxic amyloid-beta(1-42) oligomers to fibrils, *Nature Structural & Molecular Biology 17*, 561-U556.

102. Jeong, J. S., Ansaloni, A., Mezzenga, R., Lashuel, H. A., and Dietler, G. (2013) Novel Mechanistic Insight into the Molecular Basis of Amyloid Polymorphism and Secondary Nucleation during Amyloid Formation, *Journal of Molecular Biology 425*, 1765-1781.

103. Bartolini, M., Naldi, M., Fiori, J., Valle, F., Biscarini, F., Nicolau, D. V., and Andrisano, V. (2011) Kinetic characterization of amyloid-beta 1-42 aggregation with a multimethodological approach, *Analytical Biochemistry 414*, 215-225.

104. Zhao, G., Perilla, J. R., Yufenyuy, E. L., Meng, X., Chen, B., Ning, J., Ahn, J., Gronenborn, A. M., Schulten, K., Aiken, C., and Zhang, P. (2013) Mature HIV-1 capsid structure by cryo-electron microscopy and all-atom molecular dynamics, *Nature 497*, 643-646.

105. Broersen, K., Jonckheere, W., Rozenski, J., Vandersteen, A., Pauwels, K., Pastore, A., Rousseau, F., and Schymkowitz, J. (2011) A standardized and biocompatible preparation of aggregate-free amyloid beta peptide for biophysical and biological studies of Alzheimers disease, *Protein Engineering Design & Selection 24*, 743-750.

106. Vivekanandan, S., Brender, J. R., Lee, S. Y., and Ramamoorthy, A. (2011) A partially folded structure of amyloid-beta(1-40) in an aqueous environment, *Biochemical and Biophysical Research Communications 411*, 312-316.

107. Venyaminov, S. Y., and Prendergast, F. G. (1997) Water (H2O and D2O) molar absorptivity in the 1000-4000 cm(-1) range and quantitative infrared spectroscopy of aqueous solutions, *Analytical Biochemistry 248*, 234-245.

108. Klein, W. L. (2013) Synaptotoxic Amyloid-beta Oligomers: A Molecular Basis for the Cause, Diagnosis, and Treatment of Alzheimer's Disease?, *Alzheimer's Disease: Advances for a New Century 3*, 49-65.

109. Wu, W. H., Liu, Q., Sun, X., Yu, J. S., Zhao, D. S., Yu, Y. P., Luo, J. J., Hu, J., Yu, Z. W., Zhao, Y. F., and Li, Y. M. (2013) Fibrillar seeds alleviate amyloid-β cytotoxicity by omitting formation of higher-molecular-weight oligomers, *Biochem Biophys Res Commun 439*, 321-326.

110. Stine, W. B., Jungbauer, L., Yu, C., and LaDu, M. J. (2011) Preparing Synthetic A beta in Different Aggregation States, *Alzheimer's Disease and Frontotemporal Dementia: Methods and Protocols 670*, 13-32.

111. Stine, W. B., Dahlgren, K. N., Krafft, G. A., and LaDu, M. J. (2003) In vitro characterization of conditions for amyloid-beta peptide oligomerization and fibrillogenesis, *Journal of Biological Chemistry 278*, 11612-11622.

112. Bakshi, K., Liyanage, M. R., Volkin, D. B., and Middaugh, C. R. (2014) Circular Dichroism of Peptides, *Therapeutic Peptides: Methods and Protocols 1088*, 247-253.

113. Sreerama, N., Venyaminov, S. Y., and Woody, R. W. (1999) Estimation of the number of alpha-helical and beta-strand segments in proteins using circular dichroism spectroscopy, *Protein Science 8*, 370-380.

114. Matos, J. O., Goldblatt, G., Jeon, J., Chen, B., and Tatulian, S. A. (2014) Pyroglutamylated Amyloid-beta Peptide Reverses Cross beta-Sheets by a Prion-Like Mechanism, *Journal of Physical Chemistry B 118*, 5637-5643.

115. Bakshi, K., Liyanage, M. R., Volkin, D. B., and Middaugh, C. R. (2014) Fourier Transform Infrared Spectroscopy of Peptides, *Therapeutic Peptides: Methods and Protocols 1088*, 255-269.

116. Eanes, E. D., and Glenner, G. G. (1968) X-ray diffraction studies on amyloid filaments, *Journal of Histochemistry & Cytochemistry 16*, 673-&.

117. Kirschner, D. A., Inouye, H., Duffy, L. K., Sinclair, A., Lind, M., and Selkoe, D. J. (1987) Synthetic peptide homologous to beta-protein from alzheimer-disease forms

amyloid-like fibrils invitro, *Proceedings of the National Academy of Sciences of the United States of America 84*, 6953-6957.

118. Wu, C., Wang, Z., Lei, H., Duan, Y., Bowers, M. T., and Shea, J.-E. (2008) The Binding of Thioflavin T and Its Neutral Analog BTA-1 to Protofibrils of the Alzheimer's Disease A beta(16-22) Peptide Probed by Molecular Dynamics Simulations, *Journal of Molecular Biology 384*, 718-729.

119. Kuznetsova, I. M., Sulatskaya, A. I., Uversky, V. N., and Turoverov, K. K. (2012) A New Trend in the Experimental Methodology for the Analysis of the Thioflavin T Binding to Amyloid Fibrils, *Molecular Neurobiology 45*, 488-498.

120. Garai, K., and Frieden, C. (2013) Quantitative analysis of the time course of Aβ oligomerization and subsequent growth steps using tetramethylrhodamine-labeled Aβ, *Proc Natl Acad Sci U S A 110*, 3321-3326.

121. Kellermayer, M. S. Z., Karsai, A., Benke, M., Soos, K., and Penke, B. (2008) Stepwise dynamics of epitaxially growing single amyloid fibrils, *Proceedings of the National Academy of Sciences of the United States of America 105*, 141-144.

122. Necula, M., Kayed, R., Milton, S., and Glabe, C. G. (2007) Small molecule inhibitors of aggregation indicate that amyloid beta oligomerization and fibrillization pathways are independent and distinct, *Journal of Biological Chemistry 282*, 10311-10324.

123. Hino, T., Tanimoto, M., and Shimabayashi, S. (2003) Change in secondary structure of silk fibroin during preparation of its microspheres by spray-drying and exposure to humid atmosphere, *Journal of Colloid and Interface Science 266*, 68-73.

124. Volles, M. J., Lee, S. J., Rochet, J. C., Shtilerman, M. D., Ding, T. T., Kessler, J. C., and Lansbury, P. T. (2001) Vesicle permeabilization by protofibrillar alpha-synuclein: Implications for the pathogenesis and treatment of Parkinson's disease, *Biochemistry 40*, 7812-7819.